JOURNAL OF NEUROTRAUMA 35:1781–1799 (August 1, 2018)

DOI: 10.1089/neu.2017.5451

Integration of Transplanted Neural Precursors with the Injured Cervical Spinal Cord

Victoria M. Spruance, Lyandysha V. Zholudeva, Kristiina M. Hormigo, Margo L. Randelman, Tatiana Bezdudnaya, Vitaliy Marchenko, and Michael A. Lane

Abstract

Cervical spinal cord injuries (SCI) result in devastating functional consequences, including respiratory dysfunction. This is largely attributed to the disruption of phrenic pathways, which control the diaphragm. Recent work has identified spinal interneurons as possible contributors to respiratory neuroplasticity. The present work investigated whether transplantation of developing spinal cord tissue, inherently rich in interneuronal progenitors, could provide a population of new neurons and growth-permissive substrate to facilitate plasticity and formation of novel relay circuits to restore input to the partially denervated phrenic motor circuit. One week after a lateralized, C3/4 contusion injury, adult Sprague-Dawley rats received allografts of dissociated, developing spinal cord tissue (from rats at gestational days 13–14). Neuroanatomical tracing and terminal electrophysiology was performed on the graft recipients 1 month later. Experiments using pseudorabies virus (a retrograde, transynaptic tracer) revealed connections from donor neurons onto host phrenic circuitry and from host, cervical interneurons onto donor neurons. Anatomical characterization of donor neurons revealed phenotypic heterogeneity, though donor-host connectivity appeared selective. Despite the consistent presence of cholinergic interneurons within donor tissue, transneuronal tracing revealed minimal connectivity with host phrenic circuitry. Phrenic nerve recordings revealed changes in burst amplitude after application of a glutamatergic, but not serotonergic antagonist to the transplant, suggesting a degree of functional connectivity between donor neurons and host phrenic circuitry that is regulated by glutamatergic input. Importantly, however, anatomical and functional results were variable across animals, and future studies will explore ways to refine donor cell populations and entrain consistent connectivity.

Keywords: interneurons; plasticity; respiration; spinal cord injury; transplantation

Introduction

Impaired breathing is a devastating consequence of cervical spinal cord injury (SCI) that significantly increases cost of care and the risk of mortality.[1–4] Injuries at high-to-mid cervical levels (C1–C4) result in the most severe deficits because the phrenic motor circuitry—controlling the diaphragm—is directly compromised, typically resulting in dependence on assisted ventilation. Although there is mounting evidence in both laboratory[5–8] and clinical[9] settings for spontaneous respiratory improvement, the extent of recovery—or functional plasticity—remains limited. The aim of the present work was to provide a source of donor spinal neurons that synaptically integrate with the injured phrenic motor circuit to enhance neuroplastic potential.

Previous studies reported by our team[5,10–12] and others[13,14] identified spinal interneurons as a potential therapeutic target for enhancing plasticity and recovery of motor function post-SCI. With a focus on the phrenic motor system,[15–17] the aim of this study was to assess whether transplantation of developing spinal tissue, inherently rich in interneuronal and glial precursors,[18–20] could contribute to repair of respiratory pathways after cervical spinal cord contusion in the adult rat. We hypothesized that these precursors would serve as a substrate to restore input to phrenic motoneurons caudal to injury.[21–23]

In this study, a suspension of dissociated E13–E14 fetal spinal cord (FSC) tissue was transplanted into the injury cavity 1 week after a lateralized cervical (C3/4) contusion. Previous work in this field has consistently demonstrated the ability for FSC tissue to survive, proliferate, and integrate with host tissue when transplanted after a SCI.[15–17,24–27] This study builds upon these findings to assess the extent of synaptic integration between donor FSC tissue and the injured spinal cord, and vice versa. Transynaptic tracing with pseudorabies virus[5,10,11,15,17] with immunohistochemistry (IHC) was used to determine the extent of connectivity between subsets of host and donor neurons 1 month post-transplantation. Specific attention was given to characterization of donor neurons and integration between donor neurons and the phrenic circuit. These outcome measures were paired with electrophysiological assessment of phrenic nerve activity

Department of Neurobiology and Anatomy, Spinal Cord Research Center, Drexel University College of Medicine, Philadelphia, Pennsylvania.

to determine the functional effect that this integration had on phrenic motor output. Here, we show that donor tissue not only receives synaptic input from the injured host, but also synaptically integrates with the host phrenic circuitry. This integration appears to be phenotypically selective and results in a functional contribution of donor cells to phrenic output 1 month post-injury and transplant.

Methods

Adult, female Sprague-Dawley (SD) rats ($n = 59$; 225–250 g) were obtained from Harlan Scientific (now Envigo, Huntingdon, UK) and housed at the College of Medicine University Laboratory Animal Resources facility at Drexel University (Philadelphia, PA) according to National Institutes of Health guidelines and approved Institutional Care and Use Committee protocols (see Table 1). All animals were acclimated to the facility for 1 week before undergoing C3/4 lateralized contusions. One week post-injury, animals were injected with either vehicle (Hank's balanced salt solution [HBSS]; $n = 12$), allogeneic (SD; $n = 19$) or transgenic (Fischer green fluorescent protein [GFP]-expressing; $n = 16$) dissociated FSC tissue, and allowed to recover for 1 month before undergoing tracing procedures ($n = 43$) and terminal electrophysiology ($n = 39$; see Table 1). Unless otherwise stated, animals were anesthetized with separate injections of xylazine (10 mg/kg, subcutaneous [S.Q.] injection); Anased®; Akorn Animal Health, Lake Forest, IL) and ketamine (120 mg/kg, intraperitoneal [I.P.] injection; KetaVed®; Vedco, St. Joseph, MO) for all survival surgeries. Immediate post-operative care included administration of Lactated Ringers solution (5 mL, S.Q.), yohimbine (1.6 mg/kg S.Q.; Yobine®; Akorn), and buprenorphine (0.025 mg/kg, S.Q.; Buprenex®; Reckitt Benckiser Pharmaceuticals, Inc., Hull, UK). A schematic diagram highlighting the methods used in this study is shown in Figure 1.

Mid-cervical (C3/C4) lateralized contusions

In anesthetized animals, a dorsal incision was made extending from C1 to C5, and overlying cervical muscles were retracted from cervical vertebrae. A partial, lateral laminectomy of the C3 and rostral C4 portions of the vertebrae was performed to expose the dorsal spinal cord and dura. A lateralized contusion injury was made on the left side of the spinal cord at C3/C4 using the Infinite Horizons pneumatic impactor device (Precision Systems & Instrumentation, Fairfax Station, VA; Fig. 1A), with a preset impact force of 200 kilodynes (KD; zero dwell time). Animals that experienced respiratory arrest post-injury were immediately intubated and placed on a ventilator. These animals were weaned from ventilator support within an hour of injury. Animals that were unable to wean within an hour post-injury were excluded from the study. Post-injury, muscle overlying the spinal cord was closed using sterile, 4-0 or 5-0 vicryl sutures and skin was closed with would clips. Each animal received a respiratory stimulant, doxapram hydrochloride (Dopram®; 5 mg/kg, S.Q.; West-Ward, Eatontown, NJ), in addition to normal post-operative care.

Fetal spinal cord tissue collection and preparation

Developing (E13–E14) embryos were collected from timed-mated SD or F344-Tg(UBC-EGFP) rats and placed into a petri dish containing HBSS (Gibco, Gaithersburg, MD; -Mg^{2+}, -Ca^{2+}). Distinct features of E14 embryos, such as average crown-rump length ($\sim$9.5–10.0 mm) and the presence of precartilaginous formations within handplates, were used to determine gestational age.[28] Any embryo smaller than 9 mm or larger than 11.5 mm (associated with E13.5 and E14.5, respectively) was excluded from the study. Average crown-rump length of F344-GFP–derived embryos used for transplantation was 9.6 ± 0.4 mm, whereas the average length of SD-derived embryos was 11 ± 0.4 mm. Though embryo sizes appeared slightly different between the two strains, other indications of gestational age (such as digit formation) were similar. The entire spinal cord was extracted from each embryo in HBSS under a laminar flow hood using a stereo microscope (S6D; Leica Biosystems, Wetzlar, Germany). Careful dissection of spinal cord tissue ensured the exclusion of meninges, dorsal root ganglia, and

Table 1. Summary of Animals Included in This Study, Included Descriptions of Contusion Injuries, Transplant Injections, Recovery Periods, Tracing Procedures, and Terminal Electrophysiology

Group	N	*Treatment*	*Immuno-suppression*	*PRV tracing*	*Additional tracing*	*Terminal electrophysiology*
1	8	SD-FSC		PRV152 to TP	—	—
2	4	SD-FSC	—	—	BED to TP	PNR + antagonists
3	7	SD-FSC	—	PRV614 to diaph	—	diaph EMG
4	10	GFP-FSC	CSA	PRV614 to diaph	—	diaph EMG
5	6	GFP-FSC	CSA	PRV614 to diaph	BDA to C1/2	diaph EMG
6	7	HBSS	—	PRV152 to diaph	—	diaph EMG
7	5	HBSS	CSA	PRV614 to diaph	—	diaph EMG

After injury, all animals used in this study were divided into three treatment groups: vehicle injection (Hank's Balanced Salt Solution; HBSS), Sprague-Dawley derived FSC transplant (SD-FSC), or F344-GFP derived FSC transplant (GFP-FSC). Total number of animals per group (*N*) are as indicated. Animals receiving transgenic (GFP) FSC along with a subset of vehicle controls were immunosuppressed daily with CSA injections. Four weeks after transplant, animals were traced with pseudorabies virus (PRV), biotinylated dextran amine (BDA), or biotin ethylenediamnine (BED) applied to either the transplant (TP) or diaphragm (diaph). Terminal electrophysiology consisted of bilateral phrenic nerve recordings (PNR) or diaphragm electromyography (EMG).

Categories from left to right: Animal ID, injury impact force (kilodynes), impact displacement (ΔX; um), assisted ventilation required (yes or no), lesion description at the time of impact, initial weight loss within 1 week post-injury (wt loss, percent of pre-injury weight lost), days subcutaneous injections of fluids were required, days oral administration of Nutrical was required, number of cells injected into lesion cavity (in millions), whether there was visible reflex of cellular material at the time of withdrawal of the injection needle, the type of cells received (source of donor tissue being Sprague-Dawley [SD] or transgenic F344-EGFP-UBC [GFP]), additional weight loss within 1 week post-transplant (wt loss, percent of pre-transplant weight lost), days subcutaneous injections of fluids were required post-transplant, days oral administration of Nutrical was required post-transplant, type of PRV used in tracing procedures (RFP-expressing 614 or GFP-expressing 152), site of PRV administration (to diaphragm [diaph] or transplant [TP]), additional tracer injected in separate procedure (biotinylated ethylenediamine [BED] or biotinylated dextran amine [BDA]), site of additional tracer injection (TP or C1/2 ipsilateral gray matter), and terminal functional testing (phrenic nerve recording; PNR).

FSC, fetal spinal cord; GFP, green fluorescent protein.

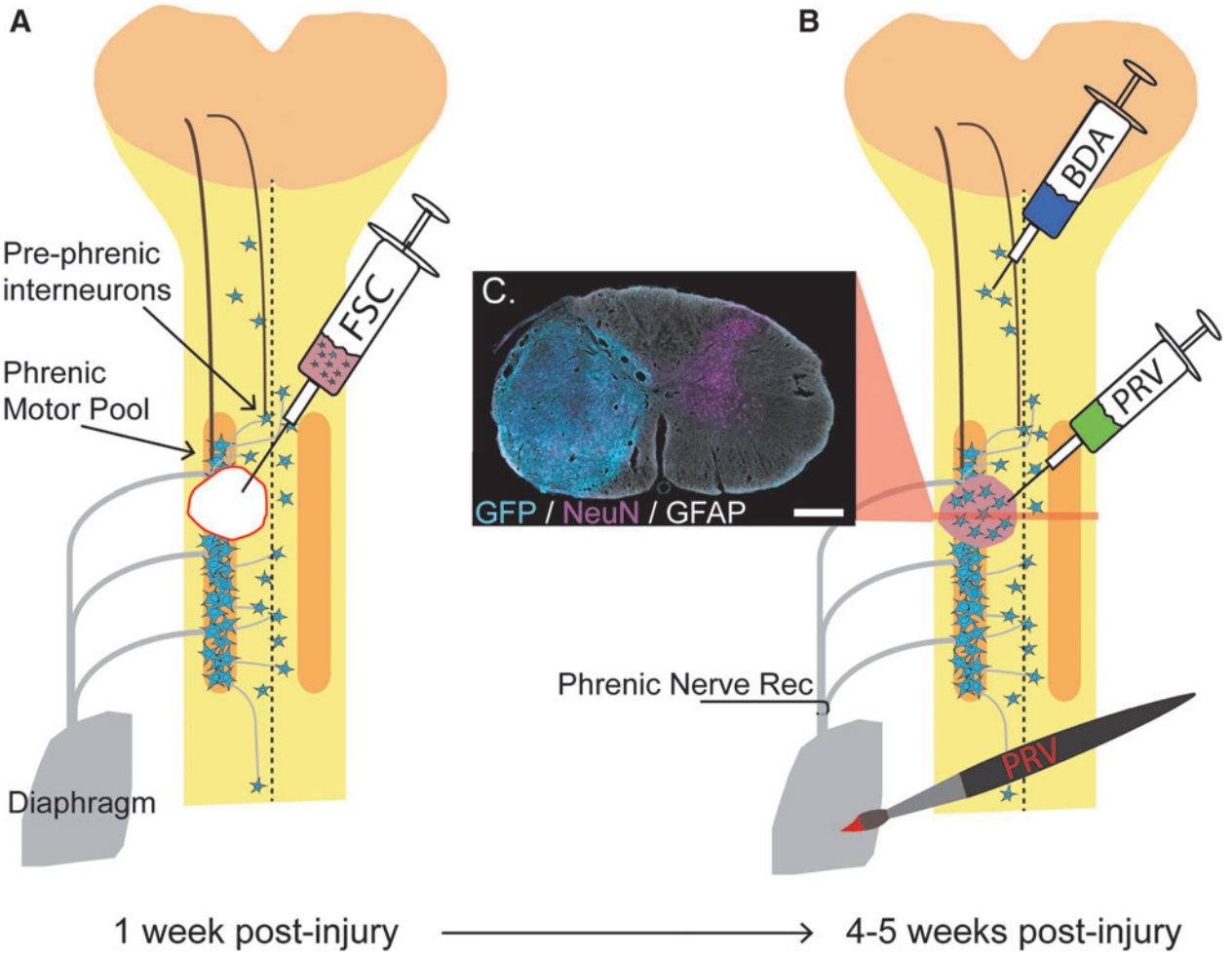

FIG. 1. Schematic of the phrenic circuit and C3/4 lateralized contusion. Respiratory drive is initiated in supraspinal neurons that project to the phrenic motor pool either directly or indirectly by pre-phrenic interneurons. Post-injury, there is compromise of descending white matter projections in addition to phrenic associated interneurons and motoneurons. At 1 week post-injury, FSC suspension is injected into the cavity at the site of injury. By 3–4 weeks after transplantation, donor neurons have survived, proliferated, and filled the cavity. A cross-section through the transplant epicenter reveals the presence of mature neurons (magenta) and glia (white) within the transplant (cyan) after immunohistochemical labeling of NeuN, GFAP, and GFP respectively (**C**; scale = 500 μm). At this point, a variety of tracing methods are used to determine host-to-transplant connectivity (BDA injection into C1/2 host gray matter or PRV injection into the transplant) and transplant-to-host connectivity (PRV delivered to the diaphragm). Terminal phrenic neurograms are conducted to determine the contribution of donor neurons to respiratory function. BDA, biotin dextran amine; FSC, fetal spinal cord; GFAP, glial fibrillary acidic protein; NeuN, neuronal nuclear protein; PRV, pseudorabies virus. Color image is available online at www.liebertpub.com/neu

any brain or brainstem tissue. It should be noted that while this tissue is typically referred to as ''fetal spinal cord'' (FSC), it is, in fact, derived from an embryonic developmental stage.[29,30] To be consistent with previously published reports,[15,16,27,31,32] and avoid confusion with ''embryonic stem cells'' (ESCs), we will also refer to our embryonic spinal cord donor tissue as FSC. Once dissected, FSC tissue was kept in clean, sterile HBSS on ice while all tissue was collected (typically around 2 h for all embryos). Strips of spinal cord tissue were then cut into smaller blocks ($\sim$12 mm in length) and were mechanically dissociated into a suspension in sterile HBSS using a 200-μL pipette (as described previously by Reier and colleagues).[26,33,34] In the absence of chemical dissociation that others have used,[3537] FSC suspensions were comprised primarily of cellular clusters rather than single cells. Cell density and viability was determined before transplantation by staining a small sample of cell suspension with trypan blue (Gibco) and manually counting cells with a hemocytometer. The minimum acceptable viability for these studies was 75%, and cell density averaged 150,185 cells/μL, $\pm$37,904 cells/μL.

Fetal spinal cord transplantation

One week after contusion, animals were anesthetized and the injury site was re-exposed. Scar tissue that had adhered to the dura at the site of laminectomy was gently removed and a small incision was made in the dura overlying the site of injury (easily identifiable because of bruising and tissue discoloration) using a 25-gauge needle. A volume of FSC suspension to include 1×10^6 cells (average = 6.5 ± 2.5 μL) was injected into the lesion cavity immediately after preparation of the cells (Fig. 1B) using a 25 μL Hamilton syringe (gastight) with a custom, 30-gauge needle (Luer-lock, 45-degree bevel), fitted into a micromanipulator (Model Kite-L; World Precision Instruments LLC, Sarasota, FL). An equal volume of HBSS was injected into the lesion cavity of control animals.

Overlying muscle was sutured and skin was closed with wound clips. Transgenic FSC recipients received daily injections of cyclosporine A (CSA; 1 mg/kg, S.Q.) beginning 3 days before transplantation and continuing through the end of the study.

Neuroanatomical tracing

Four weeks after transplantation, animals were anesthetized (2 L/min of 4% isoflurane in 100% O_2 to induce anesthesia, 2.5% isoflurane to maintain; South Medic Inc., Barrie, Ontario, Canada) and underwent a laparotomy to expose the abdominal surface of the diaphragm. A retrograde, transynaptic tracer (PRV614 Bartha strain; encoding for expression of red fluorescent protein; 50 μL, titer $1.8\times10^{10;}$ University of Florida Vector Core, Gainesville, FL) was topically applied to the entire surface of the ipsilateral, hemidiaphragm (72 h before sacrifice, as previously described[11]) to trace donor neurons synaptically integrated with host phrenic circuitry. In a subset of these animals ($n=6$), 1 μL of biotinylated dextran amine (10,000 molecular weight [MW]; 5% [w/v] in sterile saline; biotin dextran amine [BDA]; Invitrogen, Carlsbad, CA) was injected into the lateral gray matter of the C1–C2 spinal cord ipsilateral to injury, 1 week before diaphragm pseudorabies virus (PRV) tracing. In a second group of animals ($n=8$), PRV152 (encoding for expression of GFP; 1 μL; titer 1.0×10^{10}) was injected directly into the transplant 72 h before sacrifice, to examine host-to-donor neuronal connectivity. All intraspinal tracer injections were made using a 10-μL NanoFil® syringe (World Precision Instruments) with a 35-gauge needle attached. Overlying muscle was sutured and skin was closed with wound clips for all tracing surgeries.

Terminal phrenic nerve recordings and analysis

Terminal, phrenic nerve recordings were made in 4 animals that had received SD-derived FSC transplants 4 weeks previously. Initially, animals were anesthetized with isoflurane (2% in 100% O_2 before transitioning to urethane [1.2 g/kg] before recording; Acros, Morris Plains, NJ), vagotomized, paralyzed (vecuronium bromide, 3–4 mg/kg/h; Patterson Veterinary Supply, Devens, MA), and mechanically ventilated. Bilateral phrenic nerve recordings were conducted using silver, bipolar hook electrodes immersed in a mineral oil base (Fisher Scientific, Fair Lawn, NJ) as previously described.[8] Mean arterial pressure, tracheal pressure, and end-tidal CO_2 were monitored throughout the experiment. Baseline phrenic nerve activity was recorded under controlled ventilatory conditions (50% O_2, balance N_2) as well as during a 5-min, continuous hypoxic challenge (10% O_2). At this point, a cocktail of glutamatergic antagonists was injected into the transplant epicenter (0.86 mm lateral from the midline, 1-mm depth) through a glass pipette (25 um optical density). The cocktail included both an α-amino-3-hydroxy-5-methyl-4-isoxazolepropionic acid (AMPA) receptor antagonist (100 nL of 5 mM of 2,3-dihydroxy-6-nitro-7-sulfamoyl-benzo[f]quinoxaline-2,3-dione; Sigma-Aldrich, Allentown, PA) and an N-methyl-D-aspartate (NMDA) receptor antagonist (100 nL of 5mM (2*R*)-amino-5-phosphonovaleric acid; (2*R*)-amino-5-phosphonopentanoate; Tocris, Bristol, UK). After a 90-min washout period, a cocktail of serotonergic receptor antagonists (serotonin [5HT] 1, 2, and 7) was injected into the same site (100 nL of 5 mM of Ritanserin; Tocris; 100 nL of 5 mM of Pimozide; Tocris). After each drug injection, phrenic activity was recorded again under both normal and challenged respiratory conditions. At the end of each experiment, 200 nL of BED (biotin ethylenediamine; Biotium, Fremont, CA) was injected to visualize the site of antagonist application and determine the extent of diffusion. BED was selected for its MW (286) to ensure accurate representation of antagonist diffusion. In a subset of animals, simultaneous phrenic nerve and multi-unit, donor neuron activities were recorded in the center of the transplant using a Carbostar-3 microelectrode (Kation Scientific, Minneapolis, MN).

Raw phrenic nerve traces were rectified (DC bias removed with a 0.1-sec window width) and integrated (T = 0.03 sec, time constant). Integrated signals were averaged over 40-sec intervals immediately before and 10–15 min after the application of drug and at the end of each respiratory challenge. The average amplitudes of phrenic bursts was determined from the averaged integrated signal for each condition. Recordings were made using LabChart software (ADInstruments, Sydney, Australia). Analysis was completed using OriginPro 2016 software (OriginLabs, Northampton, MA).

Terminal diaphragm electromyography recordings and analysis

Terminal, bilateral diaphragm electromyography recordings were conducted as previously described (Lane and colleagues, 2012).[5] At 5 weeks post-injury (4 weeks post-transplantation), rats were anesthetized with xylazine and ketamine, as described above ($n=35$). All fur was shaved from the abdomen and neck, and the MouseOx Plus® neck cuff sensor was used to monitor pulse oximetry for the duration of the experiment (STARR Life Sciences Corp., Oakmont, PA). MouseOx data were also integrated a CED digitizer and integrated with Spike2 recording. Rats were placed in the supine position on a thermal heating pad and allowed to rest until recorded oxygen saturation was stable >95%. At this point, a laparotomy was performed to expose the diaphragm. Two electrodes (PFA-coated tungsten wire; A-M Systems, Inc., Sequim, WA) were inserted into each hemidiaphragm, in the medial portion of the costal muscle near the lateral branch of the inferior phrenic artery. Care was taken to ensure equidistant and symmetrical placement of electrodes. Baseline activity was recorded for ten minutes before administering a 5-min respiratory challenge—hypoxic gas (10% O_2, balance N_2) delivered through a nose cone at a rate of 2 L/min. After challenge, animals were immediately perfuse-fixed. All recordings were amplified (A-M Systems Differential AC amplifier, Model 1700), digitized (Power3 1401 digitizer; Cambridge Electronic Design, Ltd. [CED], Cambridge, UK), and recorded using Spike2 software (version 7; CED). Analysis was performed as described above using OriginPro software (OriginLabs). Briefly, signals were integrated and 40-sec averages of bursting activity were taken from the end of baseline and hypoxia challenge. Amplitude was calculated from the averaged, integrated signals, and two-tailed *t*-tests were used to determined significance between corresponding treatment groups.

Tissue collection and histology

A lethal dose of pentobarbital sodium and phenytoin sodium (0.4 mL, I.P.; Euthanasia Solution, Vedco Inc., St. Joseph, MO) was given to each animal, and after loss of corneal reflex and respiratory arrest, an incision was made through the thoracic cavity to expose the heart. Animals were intracardially perfused with 0.9% saline solution, followed by intracardial fixation with 4% paraformaldehyde (PFA) in 0.1 M of phosphate-buffered solution (PBS). Spinal cord and brain tissue were dissected and post-fixed in 4% PFA before being transferred to a cryoprotectant solution (15–30% sucrose in PBS). Spinal cords were embedded in Optimal Cutting Temperature compound (Tissue-Tek®; Andwin Scientific, Schaumburg, IL; free-floating sections) or M1 Embedding-Matrix (ThermoFisher,

Waltham, MA; on-slide sections) and frozen sections (25–40 um thickness, longitudinal and cross-sections) were cut using a cryostat (Leica Biosystems). IHC was completed using primary antibodies against PRV (1:10,000; courtesy of Dr. Lynn Enquist at Princeton University), GFP (1:750; Abcam, Cambridge, UK), choline acetyl transferase (1:200; EMD Millipore, Billerica, MA), serotonin (1:500; Immunostar, Hudson, WI), c-fos (1:500; Santa Cruz Biotechnologies, Dallas, TX), neuronal nuclear protein (NeuN; 1:500; EMD Millipore), glial fibrillary acidic protein (GFAP; 1:5000; EMD Millipore), tyrosine hydroxylase (TH; 1:500; EMD Millipore), glutaminase (1:100; Abcam), rat endothelial cell antigen (RECA) 1 (1:100; Bio-Rad, Hercules, CA), and glutamate decarboxylase 65/67 (GAD65/67; 1:5000; EMD Millipore). All sections intended for bright field microscopy were labeled with a biotinylated secondary antibody, followed by application of avidin-biotin complex (Vectastain ABC Kit; Vector Labs, Burlingame, CA) and enzyme substrate (DAB [3,3′-diaminobenzidine]; Sigma-Aldrich) to visualize staining. Fluorescent sections were cover-slipped using aqueous mounting medium (Fluoromount G®; Southernbiotech, Birmingham, AL; or Dako Fluorescent Mounting Medium, Dako North America, Carpinteria, CA), and bright field sections were counter stained with Cresyl Violet and cover slipped with nonaqueous mounting medium (Richard-Allan Scientific, Kalamazoo, MI). All images were taken using Zeiss Imager M2 with Apotome.2 and Zen Blue software (Carl Zeiss, Oberkocken, Germany).

Anatomical analysis

All morphometric analyses were completed on images obtained from the Zeiss Imager M2 microscope. Investigators were blinded to animal identity throughout analysis. Quantification of PRV- and choline acetyltransferase (ChAT)-positive cells were completed manually from images as described previously.[11] Briefly, PRV- and ChAT-positive neurons were identified in every other section (horizontal, 40 um thick) as having neuronal morphology and positively labeled cytoplasm with a visible nucleus. Total number of positively ChAT-labeled cells was estimated by multiplying the summed raw counts by a factor of 2. An Abercrombie correction factor was applied to raw counts to account for cells that may have been split between histological sections and counted twice. The size of ChAT-positive cell bodies was also measured using the Feret's diameter in Image J (NIH, Bethesda, MD).

Quantitative measurements of transplant and lesion cavity volume were made in recipients of GFP transplants using ImageJ. The area of GFP-positive tissue in every section was selected using a color threshold with the following parameters: hue (60–110), brightness (50–max). Area measurements were multiplied by the section thickness (40 um) and added together for a volume estimation.

Axonal outgrowth was quantified using selected longitudinal sections (40-um thickness) from GFP-transplant recipients that had been IHC labeled for GFP to enhance the signal. Three sections from each animal (one each through the dorsal horn, intermediate gray, and ventral horn) were imaged using consistent settings for Z-stack (5 slices), magnification (20×), and Apotome.2 (5-phase with phase correction and weak deconvolution). Area of GFP-positive fibers was measured at multiple points along the length of the section, beginning at each transplant edge (both rostral and caudal) and continuing at 4-mm intervals throughout the rest of the cervical spinal cord. At each measurement point, area of GFP-positive signal was measured as described above for a 300-um-length section spanning the width of the whole cord. Histograms showing changes in axonal density as a factor of distance from the transplant were generated using Origin Pro Software. Nonparametric statistical analyses included multiple, pair-wise comparisons with a significance level of 0.05 and were completed using SigmaPlot (Systat Software, Inc., San Jose, CA).

Results

Injury, animal survival, and inclusion criteria

As recorded by the Infinite Horizons Spinal Cord Impactor Software, the actual impact force across all animals averaged 228 ± 49 KD, with an average displacement of 1260 ± 676 μm (see Table 1). Post-injury, 55% of animals had minor or no subdural bleeding at the site of impact, 30% had moderate subdural bleeding, and 15% had severe subdural bleeds that obscured the laminectomy, suggesting large blood vessel disruption. All animals had moderate-sized, lateralized bruising at the center of the laminectomy immediately post-impact. Within 1 min, 94% of animals experienced respiratory arrest and were immediately intubated and ventilated, with an 89% success rate of weaning animals from ventilation within 1 h. Of the 59 animals that received injuries, 47 were included in data analysis. Reasons for study exclusion included inability to wean animals from the ventilator ($n=5$; 8%), loss of animals in the first 24 h post-injury ($n=6$; 10%), likely attributed to respiratory arrest during sleep,[38,39] and respiratory failure during terminal electrophysiology experiments ($n=1$; 2%). Post-injury, animals were treated with twice-daily fluids and Nutrical for 3–7 days, depending on individual recovery and ability to eat and drink independently. Post-injury weight loss averaged 16 ± 4% of original weight and was generally recovered by 2–3 weeks post-injury (1–2 weeks post-transplant). Nearly all animals presented with left forelimb deficits with varying degrees of paresis. Additionally, some animals exhibited hyperextension of the ipsilateral fore- or hindlimbs in the first week post-injury ($n=12$; 26%).

Transplant survival, maturation, and proliferation

Donor cell survival and confluency with host tissue was markedly better in animals receiving SD-derived donor tissue, compared with those receiving cyclosporine immunosuppression and transgenic Fisher-344/GFP–derived tissue. Consistent with previous reports,[21,33,40,41] all SD-derived FSC transplants filled the cavity and were confluent with host gray matter and, to a lesser extent, with host white matter (Figs. 1C and 2A). Of the 16 animals that received Fisher GFP-positive donor tissue, $n=12$ (75%) had evidence of macrophage infiltration, some degree of cyst formation, and modest confluency with host spinal cord. Qualitatively, the ventral, caudal transplant-host tissue interface was less confluent than observed in Sprague-Dawley transplants. Despite this, only 1 animal showed extensive transplant rejection (only small islands of transplant remaining). However, there was also evidence of neuron survival (specifically, cholinergic neurons) in this remaining tissue.

Immunostaining for NeuN (Fox3) and GFAP revealed evenly distributed neurons and glia (Fig. 2A–E), as opposed to the distinct regions of cytoarchitecture resembling adult spinal cord, that develop after nondissociated tissue transplantation into section injuries.[15,42] However, substantia gelatinosa–like areas were still observed, marked by tightly clustered regions of smaller neurons (<10 um in diameter) as previously reported.[43] Some ongoing proliferation was evident in donor tissue 1 month post-transplantation, indicated by a modest degree of Ki-67–positive neurons and glia (Fig. 2F–I). Transplants appeared to be well vascularized, after IHC analysis of RECA-1 (Fig. 2L,M). Serotonergic axons were also

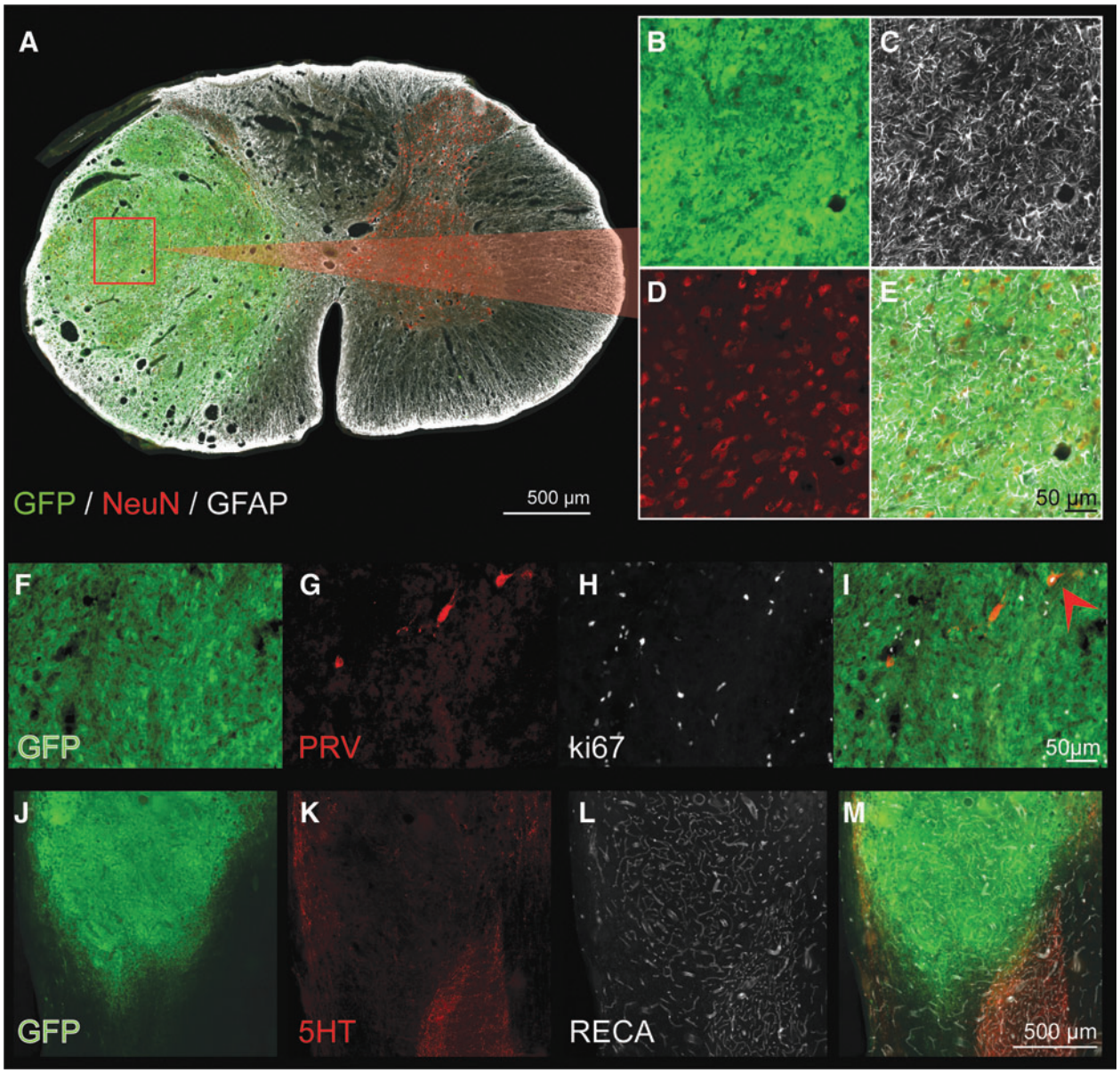

FIG. 2. Cross-section through the epicenter of a GFP-FSC transplant, 4 weeks after grafting. Donor tissue has filled the cavity, become confluent with host gray matter and contains mature astrocytes (white) and neurons (red), seen at high power in (**C**) and (**D**), respectively. In a different donor recipient, Ki-67 immunohistochemistry reveals a large number of cells still actively dividing at 1 month post-transplant (**F–I**). Whereas Ki-67–positive cells likely include both neurons and glia, one dividing, PRV-positive neuron (retrogradely labeled from the host phrenic motor pool) is visible (red arrow, I). (**J–M**) Transplanted tissue is well vascularized, and blood vessels appear to be continuous with those in the host, as seen by RECA immunolabeling (L, white). Scale is 500 um (**A**), 50 um (**B–E**), 50 um (F–I), and 500 um (J–M). 5HT, serotonin; FSC, fetal spinal cord; GFAP, glial fibrillary acidic protein; GFP, green fluorescent protein; NeuN, neuronal nuclear protein; PRV, pseudorabies virus; RECA, rat endothelial cell antigen. Color image is available online at www.liebertpub.com/neu

observed within donor tissue (Fig. 2K,M), although to a limited extent compared with host spinal cord immediately rostral to the transplant. Donor tissue contained blood vessels ranging in diameter ($\sim$5–50 μm), as observed in neighboring host tissues. The density of vasculature throughout the transplant closely resembled that of host gray matter.

Host to transplant connectivity

Anterograde tracing techniques were used to determine the extent of direct, descending, short distance (1–2 segments) propriospinal ingrowth to all donor neurons. In a subset of animals, a 1-μL injection of BDA (anterograde tracer) was made in the ipsilateral gray matter of C1/C2, rostral to the transplant. The site of injection was assessed post hoc to determine spread of the tracer. After visualizing the tracer with fluorescent antibody, it was clear that most descending BDA-labeled axons came to a stop at the host-transplant border. Only a few BDA-positive fibers appeared to penetrate the transplant and extend into the transplant epicenter (Fig. 3A,B). A similar distribution of serotonergic axons was observed throughout transplant recipients (Fig. 3C,D), as discussed below.

Given the limited growth of supraspinal axons into the transplant, retrograde, transynaptic tracing was used to map both proprio- and supraspinal neurons that innervate to donor tissue.

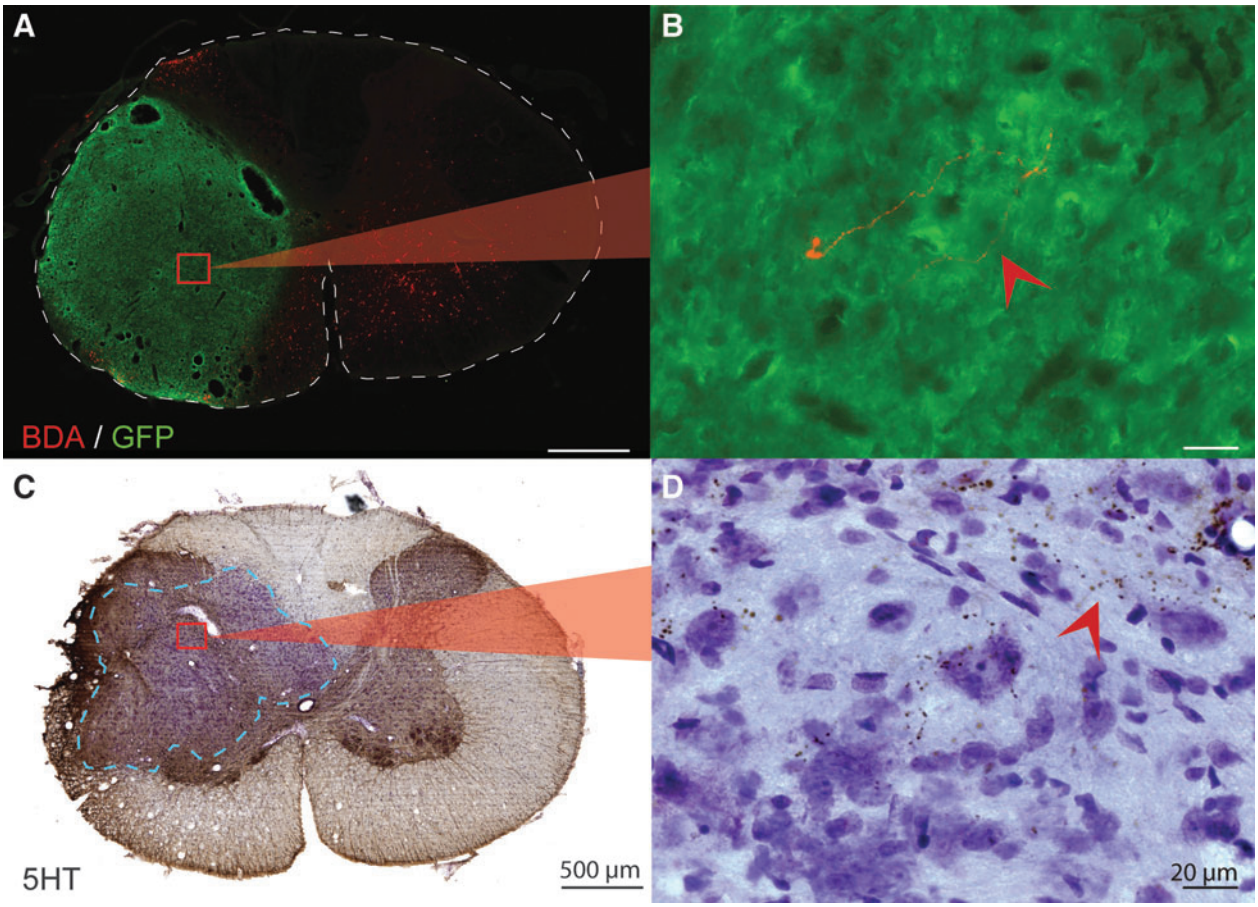

FIG. 3. Host to donor connectivity. (**A**) After injection of 1 μL, 10,000 molecular-weight BDA into the ipsilateral host gray matter at C1/2, a few BDA-positive fibers (red) can be seen near the center of the transplant (green). High magnification of a BDA fiber is seen in (**B**). (**C**) Cross-section through the epicenter of the transplant that has been immunohistochemically stained for the presence of serotonin and counterstained with cresyl violet. (**D**) A high-magnification image shows host serotonergic axons innervating the transplant near the graft-host border. Scale is 500 um for low power images (A and C) and 20 um for high-power images (B and D). Dashed lines outline the cross-section of the spinal cord (A) and delineate the graft-host border (C). 5HT, serotonin; BDA, biotin dextran amine; GFP, green fluorescent protein. Color image is available online at www.liebertpub.com/neu

Seventy-two hours after the injection of PRV into the transplant, PRV-labeled host neurons were identified throughout the cervical spinal cord (C1–C8) and brainstem (Fig. 4). Whereas host interneurons were retrogradely labeled in all animals, the extent of labeling was variable between animals in both quantity and stage of infection. The host, interneuron labeling depicted in Figure 4A–D was limited and represented early-stage PRV infection, or higher-order labeling (marked by an absence of surrounding, labeled mononuclear cells).[11] Qualitative assessment of thoracic spinal cord tissue also revealed positively labeled host spinal interneurons (figure not shown). Neuronal labeling within regions of the brainstem was highly variable with each transplant recipient, with some individuals showing bilateral labeling in multiple nuclei throughout the brainstem and others demonstrating a complete absence of supraspinal labeling. Some degree of PRV labeling was observed in 5 of 6 recipients, with the most frequent sites of PRV-positive neurons being the ipsilateral, reticular nuclei and hypoglossal nucleus. Other notable areas of labeling included the raphe nucleus, spinal trigeminal nucleus, and the solitary tract nucleus. Although there was also variability in stage of infection of positively labeled cells within the brainstem, most appeared to be in the early stage of viral infection (thus higher-order labeled, and likely indirectly connected to the transplant by polysynaptic pathways; Fig. 4E,F). The discrete injection site within the transplant can be seen in the complete horizontal section in Figure 4A (yellow arrowhead). Additionally, the enlarged image of transplanted cells at a site away from PRV injection (Fig. 4C, red arrowheads) reveals labeling in a portion of donor neurons, demonstrating intratransplant connectivity. It should be noted that most cells within the transplant were not PRV positive, thereby negating PRV diffusion as a caveat. This is consistent with parallel studies conducted by our research team that have shown PRV to be limited to a small number of neurons at the injection site 24 h post-injection (before transneuronal transport). Together, these results demonstrate that PRV-labeled supraspinal and spinal host neurons can synaptically integrate with donor interneurons.

To investigate direct, supraspinal input to donor neurons, serotonergic axons extending from the raphe nucleus into the cervical spinal cord were IHC labeled. When isolating developing spinal cord tissues for transplantation, great care was taken to exclude the medulla and thus avoid contamination by serotonergic cells. Even so, post-hoc analyses of GFP-FSC transplant recipients revealed serotonergic neurons in all recipients, as has been reported in previous studies.[16,44] Analysis of the extent of 5HT input to transplants

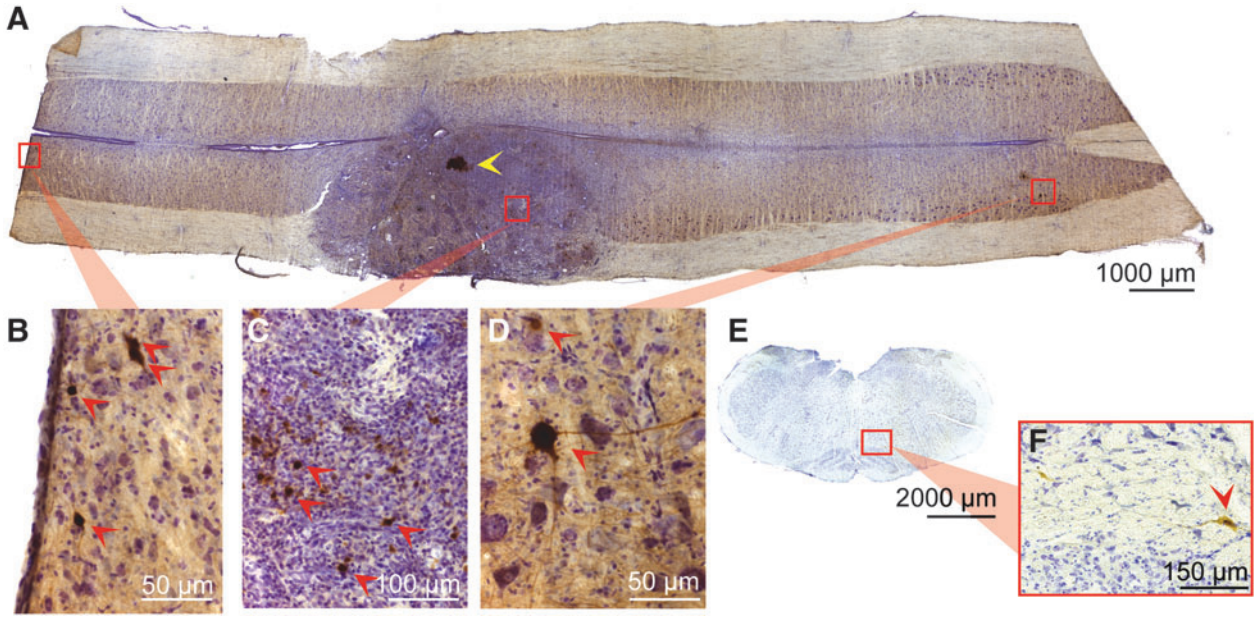

FIG. 4. Longitudinal section through the injury epicenter after injection of PRV into the transplant (**A**). The discrete injection site is denoted with a yellow arrow. A high degree of PRV-positive cells (indicated with red arrows) can be seen within the transplant (**C**), demonstrating the high degree of interconnectivity between grafted neurons. PRV labeling of host neurons is seen throughout the cervical spinal cord, from C1 (**B**) through C7 (**D**). In addition, labeling is seen within various nuclei in the brainstem (**E**), including the reticular nucleus (**F**). Orientation is rostrocaudal (left to right, A–D), dorsal ventral (top to bottom, E and F), and scales are as indicated. PRV, pseudorabies virus. Color image is available online at www.liebertpub.com/neu

was therefore limited to SD FSC recipients that showed no evidence of donor 5HT-positive neurons. In those animals, 5HT fibers accumulated within host gray matter immediately rostral to transplants with some axons extending into peripheral regions of the grafts (Fig. 3C,D).

Transplant to host connectivity

The use of F344-Tg(UBC-GFP)-derived FSC tissue enabled differentiation between host and donor neurons, and assessment of donor neurite outgrowth and donor cell migration. As seen in Figures 5A and 6A, GFP-positive (+) fibers (putative dendrites or axons) can be seen extending rostrally and caudally into the ipsilateral host white matter throughout the entire cervical spinal cord, demonstrating robust outgrowth. Importantly, GFP fibers can be seen extending to and throughout the host phrenic motor pool, the target of interest (Fig. 6A,F–I). In a subset of animals ($n=4$), GFP^+ outgrowth from the transplant was quantified at various points along the cervical spinal cord (Fig. 5). Because there was no statistically significant difference between the overall amount of outgrowth in dorsal, intermediate gray, or ventral regions, they were combined for analysis. There was a greater number of GFP^+ fibers ($p=0.007$) exiting the caudal end of the graft and extending into host gray and white matter, than observed from the rostral transplant border (Fig. 5). There was also a progressive reduction in detectable GFP^+ neurites with distance from the transplant. The number of GFP^+ neurites extending 4 mm rostral from donor tissue (to approximately C1) was significantly reduced ($p=0.009$). This represents a 78% decrease from the edge of the transplant border. Similarly, there was an 83% decrease in GFP^+ fibers found 4 mm ($p=0.006$) and 94% decrease 8 mm ($p=0.005$) from the caudal border of the transplant, representing approximately C6 and C8 respectively (Fig. 5). It is likely that GFP^+ fibers closest to transplant are comprised of both dendrites and axons, whereas those further away (several segments) are considered putative axons (Fig. 5A,B). Thus, quantified changes in neurite number needs to be carefully interpreted with this in mind. In all animals, donor glial migration can be observed extending into the dorsal- and ventral-most regions of intact, host medial white matter, as well as into the lateral white matter. There was no evidence for migration of GFP^+ neurons in the present study.

After application of PRV to the diaphragm 72 h before sacrifice, IHC revealed PRV-positive neurons within the host phrenic motor pool (first-order labeling; Fig. 6A,F–I), as well as within host cervical spinal cord and transplant (higher-order labeling; Fig. 6A,B–E). PRV labeling of transplanted neurons often occurred in clusters and were often found in the ventral portions of the transplant. In transplants that appeared to contain partitions, PRV-positive neurons could be found in all areas of the transplant. However, some partitions contained a higher number of labeled cells than others (example, Fig. 8A). Quantitative analysis of labeled cells within donor tissue revealed variability between animals (average of 235 ± 171 PRV-positive cells per transplant), though only one transplant showed no evidence of PRV-positive neurons (Fig. 8E). Interestingly, the number of donor neurons synaptically integrated with host phrenic circuitry appeared to be independent of the size of the transplant ($R^2=0.43$; Fig. 8G). Transplant-to-host connectivity was evident in both cyclosporine A (CSA; Figs. 5 and 8) and non-CSA treated animals (data not shown).

Heterogeneity of donor neuronal phenotypes

IHC revealed a wide variety of cellular phenotypes within the mature transplant that varied with each animal. Subsets of donor neurons were positively labeled for ChAT, TH, as well as GAD65/67, indicating the presence of both excitatory and inhibitory

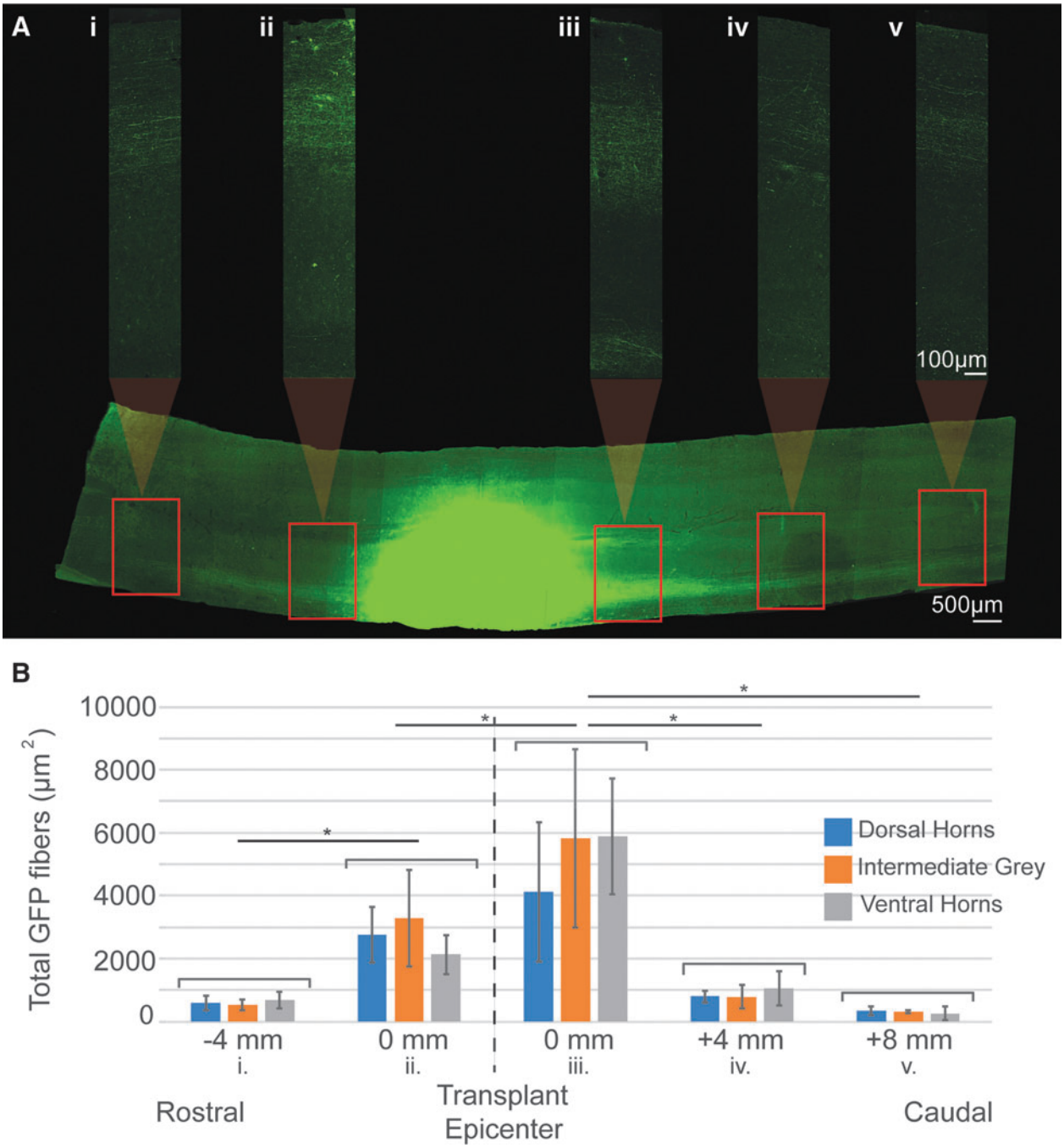

FIG. 5. Quantification of donor neurite outgrowth. A longitudinal section of the cervical spinal cord through the intermediate gray matter, immunohistochemically stained for GFP can be seen in (**A**). The transplant epicenter (green) has been overexposed so that GFP^+ neurites projecting throughout the spinal cord can be visualized. High-magnification images of GFP^+ neurites using lower, appropriate exposures were taken at 4-mm intervals along the length of the entire section, beginning at the rostral and caudal borders of the transplant and excluding GFP^+ neurons. These images spanning the entire width of the cord were used to quantify the total area of GFP^+ fibers (**B**). Outgrowth was measured in three sections per animal to include the dorsal horns (blue), intermediate gray (orange), and ventral horns (gray). Column graphs represent the average outgrowth at each distance in $n=4$ animals with standard deviation. Statistical significance is marked by asterisks ($p<0.05$). Scales are as indicated. GFP, green fluorescent protein. Color image is available online at www.liebertpub.com/neu

neurons, respectively. The apparent majority of donor neurons appeared to be glutaminase positive, apart from a few, clustered smaller diameter neurons (Fig. 7A–E). Accordingly, significantly fewer GAD65/67-positive neurons could be found throughout the transplant. However, the GABA-ergic terminal marker, GAD65/67, was present throughout the transplant as positively labeled puncta, though in varying densities (Fig. 7H,I). Cell body markers (ChAT and TH) appeared to be distributed evenly among the transplant, despite the presence of partitions in several grafts (see Fig. 7F,G for TH labeling, Fig. 8 for ChAT labeling).

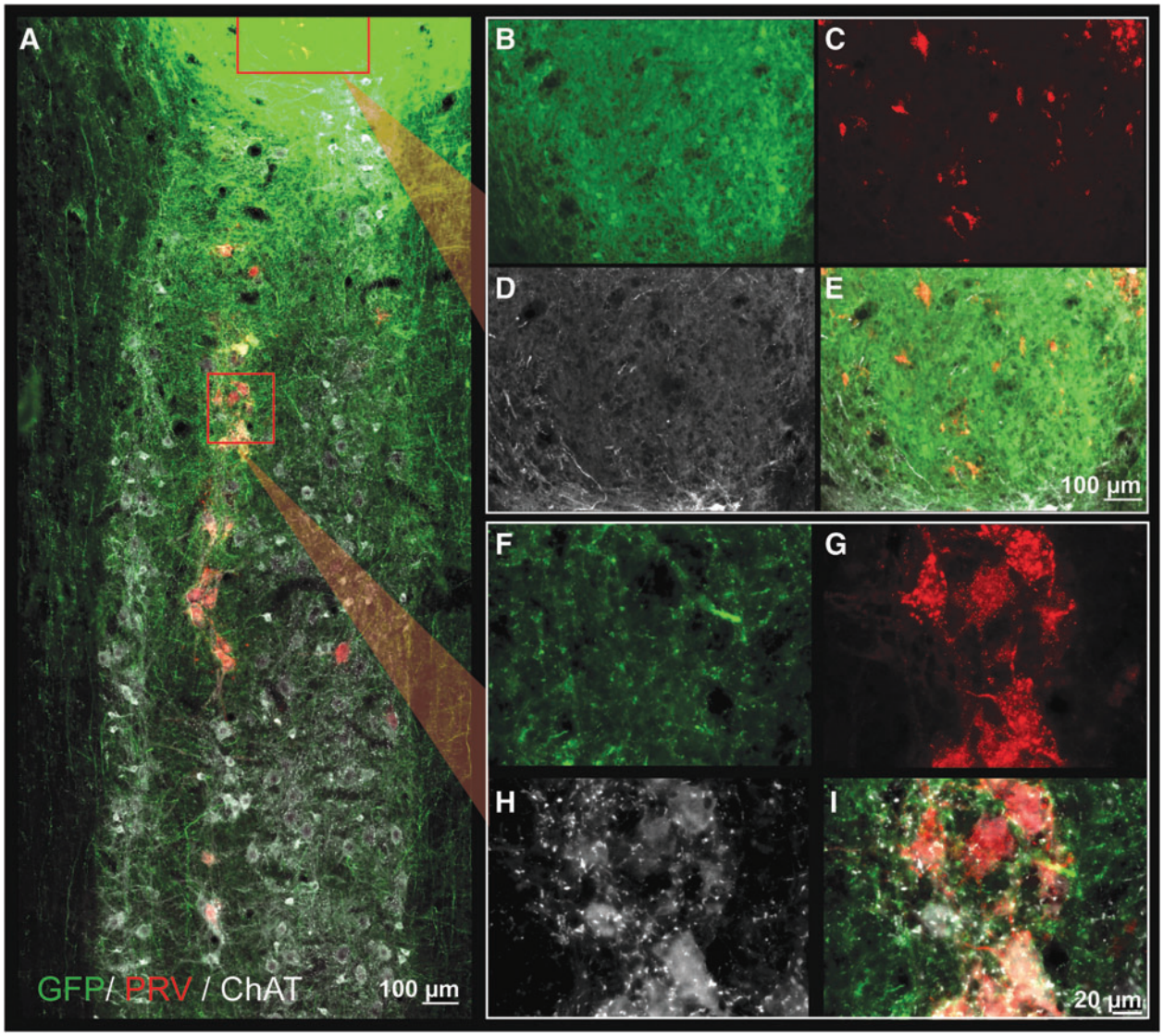

FIG. 6. Longitudinal section through the transplant epicenter and phrenic motor pool with immunohistochemical labeling of GFP (green), PRV (red), and CHAT (white) after PRV application to the diaphragm. GFP^+ (donor) neurites can be seen extending throughout the entire pictured cervical cord, from C4 to C6 (**A**). PRV labeling is seen within the host phrenic motor pool in close association with GFP axons (high magnification images seen in **F–I**) as well as within the transplant (**B–E**), indicating connectivity between donor neurons and host phrenic circuitry. Rostrocaudal orientation is top-bottom; scales are as indicated. ChAT, choline acetyltransferase; GFP, green fluorescent protein; PRV, pseudorabies virus. Color image is available online at www.liebertpub.com/neu

Given the presence of cholinergic spinal interneurons in the host phrenic circuit in naïve, uninjured animals (Supplementary Fig. 1) (see online supplementary material at http://www.liebertpub.com), we investigated the extent of donor ChAT connectivity to phrenic circuitry in a subset of animals by quantifying the number of PRV^+/$ChAT^+$, dual-labeled cells within the transplant. Although the number of ChAT donor neurons quantified in each recipient differed, there was a positive correlation ($R^2 = 0.90$) with the size of the transplant (Fig. 8F). Quantitative analysis revealed that, on average, very few (2.9%; 6 ± 6 cells) ChAT donor interneurons become integrated with host-phrenic circuitry (identified as dual PRV- and ChAT-labeled neurons) compared to the overall, high number of ChAT-positive cells (202 ± 71) present within the transplant (Fig. 8E). This relatively small number of $PRV^+/ChAT^+$ dual labeled donor cells also represents a small portion (2.5%) of the total number of donor neurons participating in host-phrenic integration, as demonstrated by the high number of PRV^+ donor neurons (235 ± 171). The average size of donor cholinergic neurons was $20.1 \pm 5.5\ \mu$m, typical of $ChAT^+$ spinal interneurons in the mature spinal cord.

In three of the four transplants with substantial PRV labeling (of those quantified in Fig. 8), less than 25% of PRV-labeled neurons were located in the dorsal half of the spinal cord (delineated by the central canal). The remaining transplant of this group had a more evenly distributed population of PRV-labeled donor neurons, with 60% located in the dorsal half of the spinal cord and 40% located in the ventral half.

Activity of donor neurons

Qualitatively, IHC revealed markedly higher levels of c-fos in donor nuclei compared to host tissue, suggesting substantial

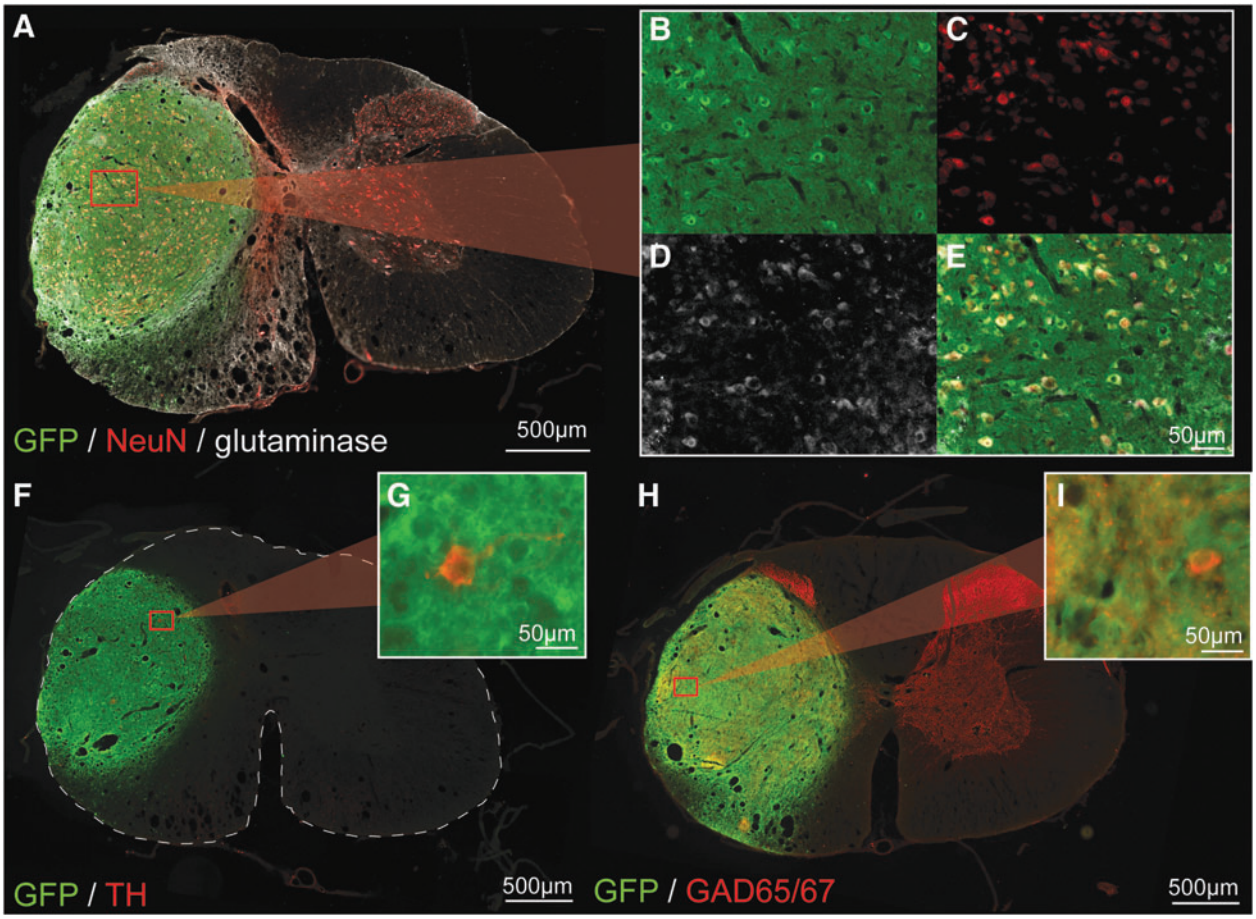

FIG. 7. Immunohistochemical characterization of transplanted neurons. Low-power images of cross-sections through the GFP$^+$ transplant epicenter can be seen in (**A**), (**F**), and (**H**), which have been immunohistochemically stained for NeuN and glutaminase (A, **B, C, D,** and **E**), TH (F and **G**) and GAD65/67 (H and **I**) in red. High-magnification insets reveal examples of glutaminase-positive, TH-positive, and GAD65/67-positive donor neurons (E, G, and I, respectively). A high degree of GAD-65/67-positive nerve terminals can be seen throughout the entire transplant, closely resembling what is seen throughout host grey matter. There are also pockets of high-density GAD-67/65 labeling in the transplant as is normally seen in the host dorsal horns, suggesting that some degree of long-term, cytoarchitecture fate is maintained. Scales are as indicated. GAD65/67, glutamic acid decarboxylase 65/67; GFP, green fluorescent protein; NeuN, neuronal nuclear protein; TH, tyrosine hydroxylase. Color image is available online at www.liebertpub.com/neu

activity within donor neurons (Fig. 9A,B). In addition, multi-unit recordings of donor cells revealed heterogeneous activity profiles, including respiratory related (Fig. 9C) and slow-wave, non-respiratory-associated activity (data not shown). An example of respiratory associated activity (Fig. 9) shows integrated traces of donor neuron activity (blue) that coincides with bilateral phrenic nerve bursting (green).

The role of serotonergic and glutamatergic inputs to donor neurons on phrenic function

To determine the contribution of host-donor and donor-host connectivity on respiratory function, phrenic nerve recordings were conducted during two separate intratransplant injections of glutamatergic and serotonergic antagonist cocktails. Average, integrated burst amplitude of ipsilateral phrenic nerves from each animal under each condition can be seen in Figure 10A,B. Example traces from 1 animal can be seen in Figure 10C,D. Phrenic nerve amplitude was smaller ipsilateral (0.13 ± 0.04 volts) than contralateral (0.30 ± 0.08 volts) to injury in all animals, though at varying degrees (data not shown). After the application of the NMDA and AMPA receptor antagonists to the transplant, 2 of 4 animals showed a substantial decrease ($-26 \pm 4\%$) in ipsilateral phrenic burst amplitude (Fig. 9C, blue and green data points), whereas the remaining 2 animals demonstrated minimal or no change ($6.7 \pm 4\%$; yellow and red data points). After delivery of a 5HT-1, -2, and -7 receptor antagonist cocktail, minimal changes in ipsilateral phrenic burst amplitude ($-1 \pm 7\%$) were seen under normal breathing conditions (Fig. 10D).

The effect of fetal spinal cord transplants on diaphragm function

Terminal electromyography (EMG) recordings demonstrated an increase in ipsilateral, hemidiaphragm burst amplitude during eupneic (baseline) breathing after SD-derived FSC transplantation ($n = 7$) compared to vehicle-injected animals ($n = 7$; $p = 0.01$; Fig. 11A). Whereas average burst amplitudes were not statistically significant between HBSS + CSA– ($n = 5$) and GFP-FSC–treated ($n = 16$) groups (both receiving CSA immunosuppression), there

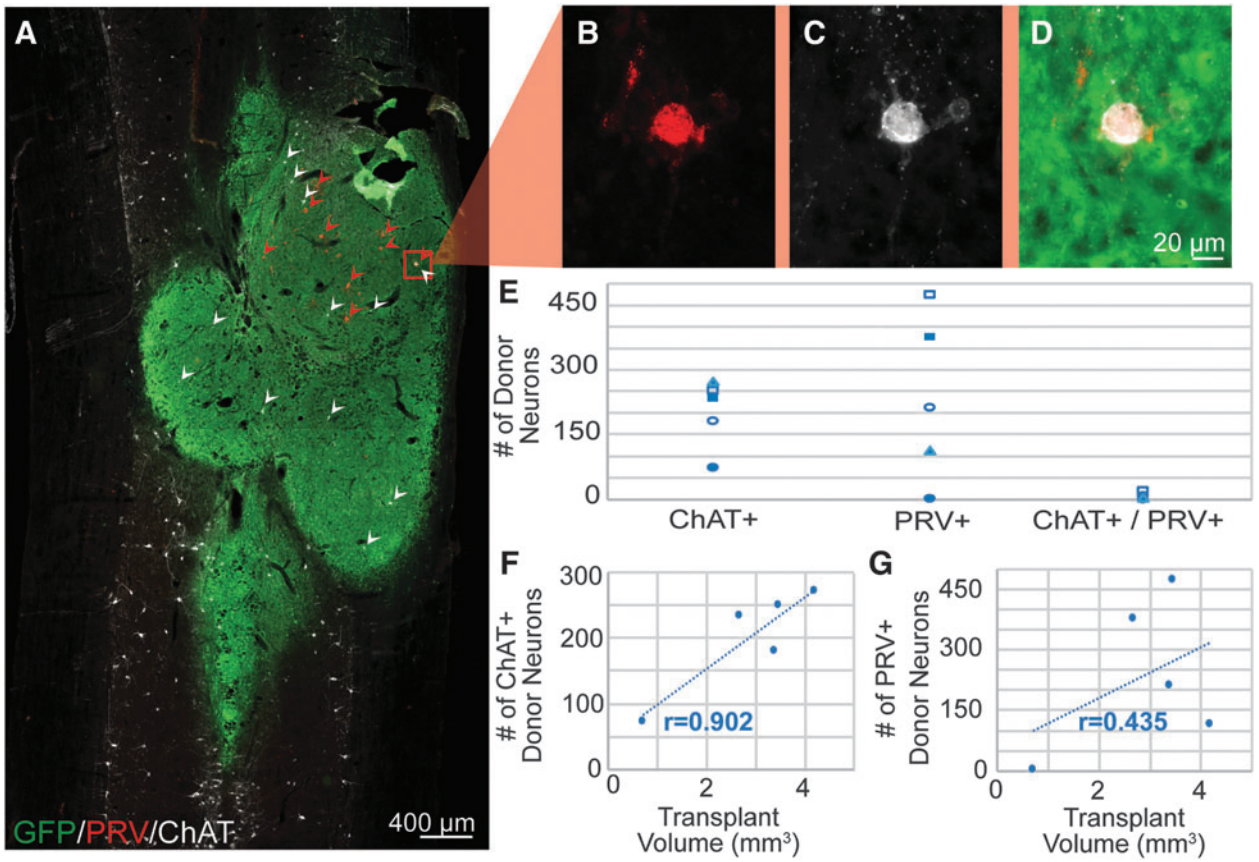

FIG. 8. Quantification of donor to host connectivity. (**A**) Longitudinal section through the transplant epicenter shows donor FSC tissue (green) that has been immunohistochemically labeled for PRV (red) and ChAT (white). A higher magnification of a co-labeled (PRV and ChAT) donor neuron can be seen in (**B**)–(**D**). Quantification of these neurons within the transplant reveals that very few $ChAT^+$ donor neurons connect to host phrenic circuitry (**E**). ChAT-positive neurons mostly appear to be evenly dispersed throughout the transplant, and the number of donor ChAT neurons correlates with the size of the transplant (**F**). Conversely, donor PRV^+ neurons often appear in clusters, and quantification appears independent of transplant size (**G**). Rostrocaudal orientation is top-bottom, and scale bars are as indicated. ChAT, choline acetyltransferase; GFP, green fluorescent protein; PRV, pseudorabies virus. Color image is available online at www.liebertpub.com/neu

was greater variability among transplant recipients as indicated by larger standard deviations. Individual data points have also been overlaid on the column graph averages to depict this increase in spread. Notably, the distribution of GFP-FSC recipients appears clustered into responders and nonresponders, where 5 of the 16 animals in this group showed greater diaphragm activity than vehicle-treated controls. Analyzed separately, these animals had significantly greater baseline diaphragm compared to vehicle controls ($p < 0.00001$).

Transplant of either SD-FSC or GFP-FSC did not seem to affect response to respiratory challenge (Fig. 11B), measured by the percent change in ipsilateral, hemidiaphragm burst amplitude from baseline to hypoxia. However, there was a large degree of variability across animals from all groups for this outcome measure.

Discussion

Building upon previous work using transplanted neural precursor cells to repair the injured cervical spinal cord, the present work, for the first time, 1) identifies subpopulations of spinal interneurons that synaptically integrate with injured phrenic motor pathways and 2) reveals that donor neurons being modulated by glutamatergic drive can contribute to phrenic motor output 1 month post-injury and transplantation.

Cell survival, confluency, and integration

As previously demonstrated,[33,34,40] FSC-derived neural precursor cells are capable of surviving, proliferating, and restoring continuity when transplanted into the site of a spinal cord contusion injury without any other intervention. The results from the present work reveal that this remains true for transplanted precursors derived from wild-type embryos of the same strain (SD), though to a lesser extent for transgenic (GFP-expressing) embryos from a different strain (Fischer344), the latter of which consequently require recipient immunosuppression. The number of cells per transplant (approximately 1×10^6) used in this study was chosen based on previous work by Giovanini and colleagues[26] that demonstrated confluency between host and donor tissue upon transplant maturation with this dose. However, few dose-response studies have been completed with FSC tissue transplants. With the expression of Ki-67 in donor neurons observed in the present work, one consideration is that, at the dose given, FSC tissue transplants may ''overproliferate'' or become tumorigenic. According to a tumorigenicity study completed by Priest and colleagues,[45] neural transplant populations containing 10% human embryonic stem cells led to teratoma formation in 13% of recipients, whereas a 1% human embryonic stem cell population did not result in any teratoma formation. Rat, E14 spinal cord tissue contains approximately

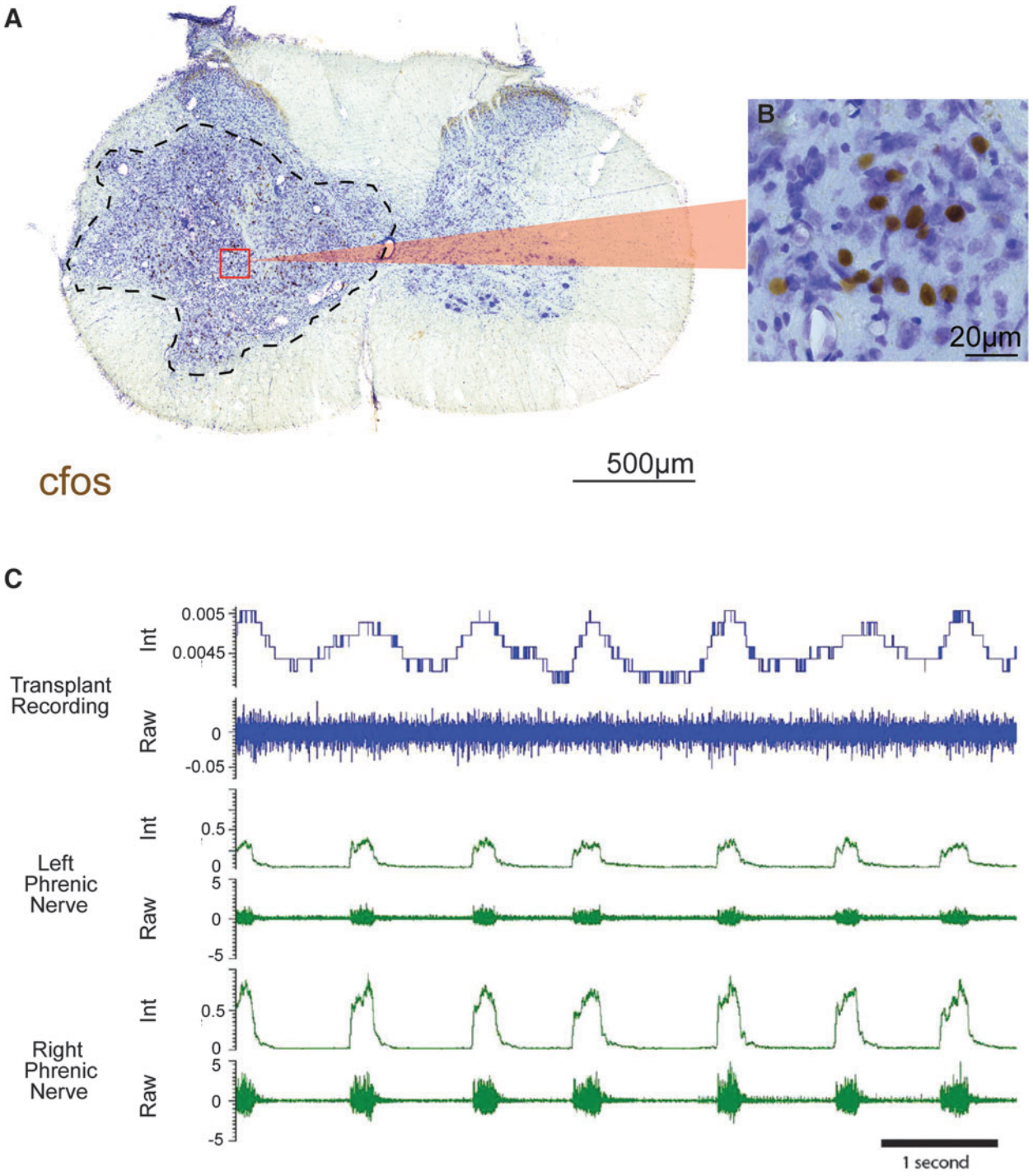

FIG. 9. Activity of donor neurons. (**A**) Cross-section through a SD-derived transplant, where dashed lines indicate the donor-host border. Immunohistochemical labeling of cfos demonstrates high degree of neuronal activity within the transplant, indicated by a large number of labeled nuclei (**B**). Multi-unit recordings of donor neuron activity revealed a bursting pattern (blue) correlated to phrenic motor output (green, **C**). Both integrated (top) and raw (bottom) activities are shown for each recording site. Scales are as indicated. Color image is available online at www.liebertpub.com/neu

5–10% of an undifferentiated neural stem cell population,[46,47] as well as a late-stage population of multi-potent, neural crest cells that persist at the dorsal root entry zone.[48] Although both populations could pose a tumorigenic risk even at relatively low concentrations, this has not been observed with FSC tissue transplantation across a range of species and injury models.[16,21,26,33,35,40,49,50] In fact, achieving adequate tissue survival is a more common concern. Regardless, future FSC studies should also pursue a more detailed dose-response study to determine whether similar results (such as confluency and integration) can be achieved with fewer transplanted precursor cells, and whether overgrowth may result from transplanting a higher number of donor progenitors. It is important to note that the sheer presence of stem cells alone is not sufficient to induce tumorigenesis. It is now recognized that the normal, intact

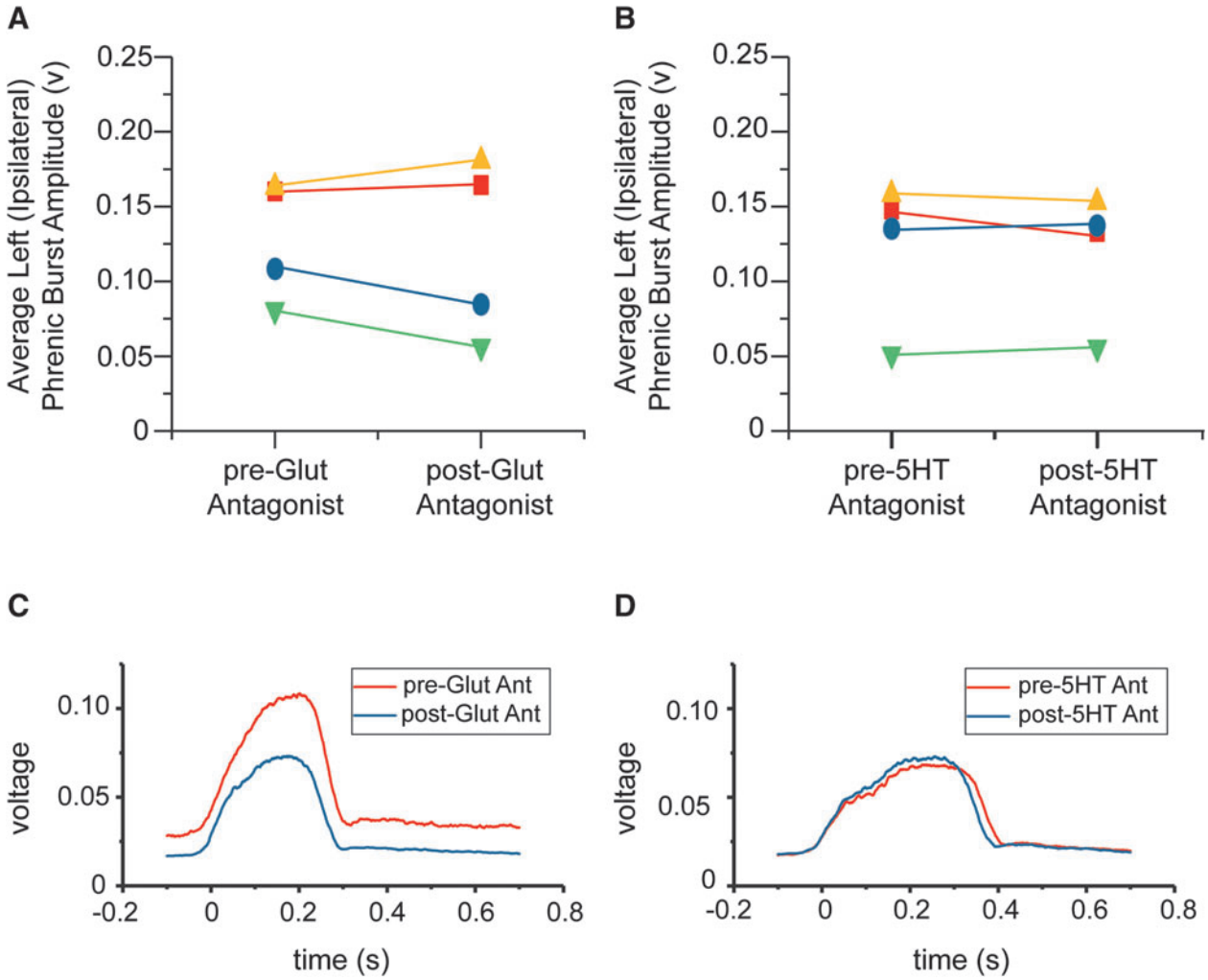

FIG. 10. Functional connectivity between donor and host phrenic circuitry. Terminal, phrenic nerve recordings were conducted to determine the extent of functional connectivity between donor and host phrenic circuitry. After collecting baseline phrenic activity, glutamatergic (NMDA and AMPA), and serotonergic (5HT-2, -5, and -7) receptor antagonists were injected directly into the transplant epicenter, separated by a washout period. The average amplitudes of left (ipsilateral to injury) integrated phrenic bursts are shown before and after application of glutamatergic (**A**) and serotonergic (**B**) antagonists to the transplant. Each point represents data from an individual animal. Changes in phrenic bursting in response to glutamatergic antagonist application was seen within 10 min in 50% of animals (blue and green, A), though minimal change was seen in response to serotonergic antagonist (B). Examples ipsilateral, integrated phrenic bursts from one animal can be seen in (**C**) and (**D**), where each trace represents a 40-sec average of phrenic activity before (red) and after (blue) antagonist application. 5HT, serotonin; 5HT Ant, 5HT antagonist; AMPA, α-amino-3-hydroxy-5-methyl-4-isoxazolepropionic acid; NMDA, N-methyl-D-aspartate. Color image is available online at www.liebertpub.com/neu

adult central nervous system (CNS) contains several populations of stem cells that most often persist without pathological consequences.[51–54] For tumorigenesis to occur, the internal processes of these cells must be deregulated, which can arise from either exogenous signaling or internally generated genetic mutations.[55] However, given previous pre-clinical[56] and clinical[57] evidence for tumor formation post-transplantation of isolated, undifferentiated neural stem cells, this risk should be carefully considered for any cell therapy that progresses toward the clinic. It is likely that purified, restricted progenitor populations are the safer alternative to eliminate this risk altogether.

Recent work using FSC transplants has raised concern over the formation of rifts or partitions in mature cell transplants within the spinal cord.[35,44,58] A portion of the transplants completed for this study showed similar gross anatomical compartmentalization of donor tissue. After transplantation of FSC suspension, there is an acute loss of most donor cells[59] followed by substantial proliferation of surviving neurons, which tend to adhere to peripheral edges of the lesion cavity. These partitions are possibly a result of surviving islands of cells around the cavity that subsequently proliferated toward one another. However, the presence of such divisions within transplants in the present work, likely defined by glial limitans,[60,61] did not prevent connectivity between donor and host neurons throughout the entirety of the graft as seen with transneuronal tracing. Therefore, it is possible that partitions may not hamper the ability for transplanted neurons to form appropriate connections that ultimately improve function.

In the present study, the cytoarchitecture within an individual transplant (or large partition) appeared more homogenous than what has previously been described for whole tissue transplants

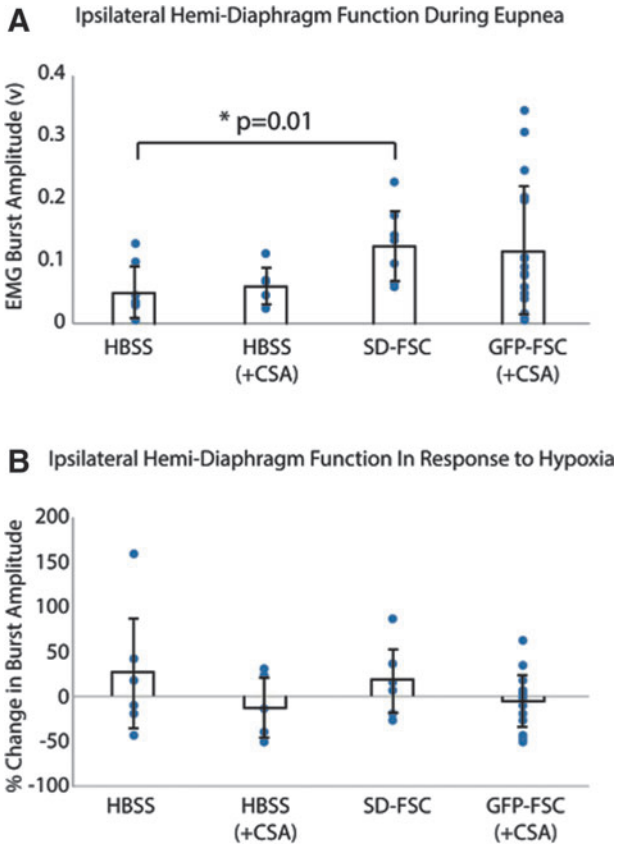

FIG. 11. Terminal, ipsilateral hemidiaphragm electromyography (EMG) activity post-injury and treatment. (**A**) Bar graphs represent the average burst amplitudes during baseline activity (± standard deviation) for each group: vehicle (HBSS) treated with or without immunosuppression (+CSA), Sprague-Dawley–derived fetal spinal cord tissue (SD-FSC) transplantation, and GFP-expressing Fisher–derived tissue (GFP-FSC) transplantation with immunosuppression (+CSA). Averages were calculated from 40-sec samples of integrated activity during eupneic (20% O_2) breathing. (**B**) The average percent changes (± standard deviation) in burst amplitude in response to a respiratory challenge (hypoxia, 10% O_2) for each group. Individual data points have been overlaid to show the extent of variability in each group. CSA, cyclosporine A; FSC, fetal spinal cord; GFP, green fluorescent protein; HBSS, Hank's balanced salt solution. Color image is available online at www.liebertpub.com/neu

(nondissociated FSC) into section lesions. Although there was evidence of substantia gelatinosa–like cell clusters, they were much smaller and fewer in number than what has been shown in nondissociated FSC transplants.[15,16,43] This may suggest that the dissociation process prevents donor neurons from retaining their long-term cytoarchitecture fate, either directly or indirectly by disrupting normal cell to cell signaling processes as development progresses.

Donor neurite outgrowth

The use of transgenic donor spinal cord tissue that ubiquitously expresses GFP allows visualization of neurite outgrowth from grafted cells into host tissue. Consistent with previous work,[16,25] the present results confirm that fetal-derived donor neurons extend neurites several millimeters rostrally and caudally throughout the cervical cord.[35,44] The present results also indicate that this type of outgrowth is possible without exogenous growth factors or co-implantation with biological matrices. Although the long-distance neurite growth demonstrated in this study is likely axonal, outgrowth nearest the transplant likely consists of both short-distance axonal sprouting and dendritic growth. At this close proximity to the host-transplant border, GFP-positive fibers are observed extending into both host gray and white matter. However, GFP fibers appear to travel mostly within white matter at farther distances along the length of the cervical cord. As expected, the highest density of neurite outgrowth is located closest to the transplant, with densities tapering as distance from the donor-site increases. One consideration is that donor neurons are likely establishing shorter distance projections with contacted host neurons and thus cease to further extend their neurites, as previously demonstrated.[25] Accordingly, they may be innervating spinal interneurons within the first few hundred microns of the transplant-host interface, which, in turn, can form polysynaptic connections with host spinal motoneurons. Given the proximity of phrenic motoneurons to the transplant, donor cells may also be innervating them directly. With this in mind, transplantation of donor neurons into the cervical spinal cord may require only very short distance outgrowth to achieve biologically relevant functional changes after cervical SCI. Most important, the present work demonstrates that donor neurons are unquestionably capable of extending neurites into the host for distances sufficient to reach the ultimate intended target-phrenic motoneurons. Within the ventral horns from C3–C5, there is high density of GFP-positive fibers observed in and around the phrenic motor pool (Fig. 6). Therefore, future studies should focus more on directing appropriate growth rather than enhancing general outgrowth from transplanted cells, given that their intrinsic growth capacity appears more than sufficient.

Integration of donor neurons with host phrenic circuitry

Previous studies have demonstrated nonspecific connectivity between donor and host neurons in the contusion model,[26,27] as well as phrenic-specific donor to host connectivity within the hemisection model.[15,16] The present work shows the potential for interneuronal progenitor transplants to form novel connections with the host phrenic circuitry after cervical contusion. In most animals, a substantial number of PRV-labeled neurons could be found in the transplant after applying PRV to the diaphragm. Whereas the degree of connectivity between donor and host neurons is variable between animals, some level of synaptic integration with the phrenic circuit was evident in every animal, including those with relatively poor graft survival. The clustered nature of PRV-positive donor neurons indicates a high degree of interconnectivity within the transplant, particularly within a single partition (see Fig. 8). Given that PRV moves in a time-dependent manner,[11] low-order labeling of donor interneurons (e.g., second or third order) may be distinguished from higher-order labeled neurons based on stage of infection. Late-stage infection, or lower-order labeling (first to second), is characterized by labeled glia in close proximity (which take up virus at the synapse), and accumulation of mononuclear cells around PRV-labeled cells. Therefore, PRV neurons with fewer surrounding labeled cells were likely infected closer to the time of perfusion. Clustered PRV-positive neurons as well non-clustered labeled neurons appeared throughout rostral and caudal portions of the transplant in this study. However, there appeared to be a higher number of labeled neurons in the more ventral portions of the transplant compared with dorsal areas, suggesting that more ventrally located donor neurons may preferentially integrate with host cervical phrenic circuit, which may be expected given the proximity to the phrenic motor pool.

Characterization of donor neuron phenotypes

FSC tissue contains a wide variety of developing neural (neuronal and glial) and non-neural cell phenotypes, and this heterogeneity is carried through to maturation. Previous work has revealed that this E14 donor tissue is comprised of approximately 30% glial restricted progenitors (A_2B_5-positive) and 60% neuronal restricted progenitors (E-NCAM positive).[47] The remaining 10% is comprised of embryonic neuroepithelial cells (proliferating, homogenous) and other non-neural elements (e.g., endothelial cells). Mature FSC transplants contain both neurons and glia, and a population of proliferating cells that persist at least 1 month post-transplantation. The neuronal phenotypes include excitatory and inhibitory interneurons. Consistent with previous work, we saw no evidence of spinal motoneurons within donor tissue, supported by the small (20 μm) size of cholinergic neurons, with no ChAT-positive neurons exceeding 30 μm. This is likely because the age at which the spinal cord is dissected (E13–E14), axons from spinal motoneurons are extending into the ventral roots and are thus are transected close to the cell body upon dissection, resulting in selective motoneuron death.[59,60] This results in neural tissues rich in a wide range of interneuronal precursors. The ability to track cholinergic (ChAT-positive) interneurons and catecholaminergic (TH-positive) neurons with IHC enabled us to focus on their distribution within the donor tissue in the present work. Assessing the distribution of other spinal interneuron subtypes[62,63] is difficult without the use of transgenic tissues.

Cholinergic interneurons appeared evenly distributed throughout the grafts, contrary to previous reports that clusters of ChAT-positive neurons develop in whole-tissue FSC transplants.[16] In the uninjured spinal cord, cholinergic neurons are found throughout the intermediate and ventral grey matter, with dense expression in the motor pools, at the delineating marker of dorsal and ventral tissues, and around the central canal.[64,65] Derived from V0 spinal progenitor populations,[63,66,67] spinal cholinergic interneurons are reported to normally project across one to three spinal segments, synapse onto Renshaw cells or directly onto motoneurons, and modulate the amplitude motor output.[63,68] Cholinergic interneurons also comprise a portion of premotor phrenic interneurons in the uninjured spinal cord (see Supplementary Fig. 1) (see online supplementary material at http://www.liebertpub.com). Thus, ChAT-positive interneurons may represent a viable donor cell type to restore modulatory input to the phrenic motor system. However, despite being present in all grafts (directly correlating with overall transplant size) and evenly distributed, ChAT-positive interneurons integrate poorly with host phrenic neurons. It is possible that these cells may be connecting to other spinal circuitries, or are simply incapable of extensive growth into the injured cord. Regardless, this raises the question for future studies: Which cells have a greater affinity for integration, and are they beneficial?

Host, propriospinal integration with donor neurons

PRV delivery to the transplant resulted in widespread labeling of host neurons throughout the cervical and thoracic spinal cord, and brainstem, consistent with previous reports of host to donor integration.[69] The distribution and extent of labeling, however, varied between animals. This may be attributed, in part, to the site of PRV injection into transplant, and number of donor cells labeled with each PRV injection. Although there was host interneuron PRV labeling at C1 (Fig. 4), anterograde BDA labeling from C1 revealed only minimal propriospinal projections to transplant. This is likely because host interneurons in closer proximity to the transplant are more apt to make connections with donor neurons than those located multiple segments away. PRV labeling in the rostral and caudal ends of the cervical cord likely represents higher-order neuronal labeling, which is supported by the early-stage PRV infection of these cells.

In addition to anatomical evidence for host-donor and donor-phrenic connectivity, electrophysiological recordings of transplanted neurons revealed bursting patterns correlated to phrenic nerve activity. Previous reports have found similar, respiratory-related activity profiles[70] after pairing transplantation with rehabilitation strategies (discussed below). Donor neuron activity in the present work also increased in response to a respiratory challenge, as previously reported.[17] Thus, it is possible that respiratory related donor neuron activity may be augmented with respiratory training.

Electrophysiological recordings from the present work demonstrated that the input to donor neurons can exert influence on phrenic output. After application of a glutamatergic (NMDA and AMPA) antagonist cocktail to the transplant, 50% of animals showed a decrease in the average, ipsilateral phrenic burst amplitude. Although there was some variability in the degree of response (increase or decrease in burst amplitude) to the antagonist application, 75% of animals showed some type of change. Similar variability in outcome was observed in terminal diaphragm EMG, especially evident in baseline burst amplitudes among GFP-FSC recipients. Nevertheless, SD-FSC recipients showed significant improvement in ipsilateral hemidiaphragm activity compared to vehicle-treated controls. This contrasts with what was recently reported by Lin and colleagues,[16] where response to challenge was improved in transplant recipients. The differences between outcome could be attributed to differences in 1) injury models used (C4 hemisection vs. C3/4 contusion) 2) or differences in donor tissues transplanted (derived entirely from SD vs. the use of Fischer-344 donor tissues).

The variability in functional outcome likely stems from the heterogeneous population of donor neurons and/or variability in connectivity. For example, White and colleagues demonstrated that FSC transplants derived from the dorsal plate may actually worsen diaphragm function after C2 hemisection.[15] Therefore, the differential survival and integration of these particular precursors in transplants derived from the entire developing spinal cord could contribute to variability in function. The conditions under which functional assessments are made may also contribute to variability in outcome (spontaneously breathing vs. ventilated, awake vs. anesthetized, or even different depths of anesthesia). Nevertheless, these electrophysiological data support the idea that short-distance sprouting may be sufficient to form functional and biologically meaningful effects on spinal circuits.

Supraspinal innervation of transplants

Modest serotonergic projections observed within the donor tissue likely originated from the host raphe nucleus (animals with 5HT-positive neurons were excluded from analysis). This suggests that not only do donor neurons synapse onto host phrenic circuitry, but they may also be receiving modulatory input from supraspinal centers. Several groups have demonstrated that serotonergic modulation is a key aspect of respiratory plasticity.[71–74] From a more translational perspective, a growing area of interest in the field of SCI and rehabilitation is the use of acute, intermittent hypoxia (IH) as a way to facilitate plasticity in respiratory (and nonrespiratory) motor circuits.[70,75] This neurorehabilitative approach has shown success in both pre-clinical[76] and clinical[77,78] studies, and its effects are thought to be mediated (in part) by supraspinal, serotonergic projections. A hypoxic episode stimulates serotonin release into the spinal cord[79] and an increase in the electrophysiological activity of mature, FSC transplanted neurons.[17] In our studies,

whereas hemidiaphragm EMG activity during baseline breathing was increased in SD-FSC recipients compared to vehicle controls, there was large degree of variability in diaphragm activity during hypoxia across transplant groups. This might be expected given this is a serotonergic-mediated response, and serotonergic innervation of transplants was modest and variable. However, whereas phrenic nerve recordings did not reveal an immediate change in baseline burst amplitude after the application of a serotonergic antagonist to the transplant, there was a subsequent diminished response to hypoxia in most animals. This may suggest that serotonergic integration with phrenic-associated donor neurons plays a modulatory role to enhance phrenic function under respiratory challenge post-injury, but will require more extensive investigation in future work. Using combined treatment with FSC transplantation and daily acute IH, Gonzalez-Rothi and colleagues[70] demonstrated that training 1) induced donor neuron bursting patterns that correlated with phrenic activity and 2) increased donor neuron activity (in a similar manner as phrenic nerve activity) during exposure to hypoxia in the terminal setting. Given this evidence and general Hebbian principles, pairing IH with neuronal cell transplantation may be a viable way to direct and maintain the appropriate host to donor connectivity that will facilitate greater respiratory improvement.

Closing remarks

The results from this study support the notion that FSC-derived interneuronal precursors can form host-phrenic-host circuits that contribute to phrenic nerve function after cervical SCI. A common theme among the results presented here, however, is variability. The number of donor neurons that connect to host circuitry, their phenotype, and the input they receive ultimately varies between animals and, not surprisingly, contributes to variable functional outcome. Refining the donor neuron population and directing growth to the target of interest will hopefully provide more consistent functional outcomes. Future work will investigate ways to direct appropriate growth between host and donor neurons (and vice versa), and maintain this growth over time.

The vast array of spinal interneuronal phenotypes, each with distinct functions in the naïve adult spinal cord, needs to be considered when transplanting neural precursors. One possibility is that treatment of distinct motor and sensory systems will require tailoring cell therapies. Given that technological advancements have allowed for the differentiation and isolation of multiple different neuronal subtypes,[80–82] individualized transplantation strategies to specifically address a unique set of post-injury dysfunctions are becoming more possible. However, in many cases (as with the phrenic circuit), the exact role that specific interneuron populations play in normal motor or sensory functioning has been unclear. As research better elucidates the neuronal networks involved with function in the normal and injured spinal cord,[10,83–85] potentially therapeutic neuronal phenotypes are being identified. Ongoing work is now beginning to explore how specific donor neurons can be harnessed, transplanted, and integrated to form new neural networks that are capable of contributing to plasticity, repair, and functional improvement post-SCI.

Acknowledgments

Research reported in this publication was supported by the National Institute of Neurological Disorders and Stroke of the National Institutes of Health under Award Number R01NS081112. The content is solely the responsibility of the authors and does not necessarily represent the official views of the National Institutes of Health. Research support also included the United States Department of Defense (CDMRP #SC140038; Marchenko), Craig H. Neilsen (#338432, Lane), the Spinal Cord Research Center at Drexel University, College of Medicine (NIH, P01 NS 055976), and the Drexel Deans Fellowship for Collaborative or Themed Research (Zholudeva). PRV614 was produced and supplied by Dr. David Bloom (University of Florida). Primary antibodies to PRV were supplied by Lynn Enquist (Princeton University) as part of Virus Center funding (P40 RR018604) awarded to Dr. Enquist. We also thank Dr. Paul Reier for his comments on the manuscript.

Author Disclosure Statement

No competing financial interests exist.

References

1. Brown, R., DiMarco, A.F., Hoit, J.D., and Garshick, E. (2006). Respiratory dysfunction and management in spinal cord injury. Respir. Care 51, 853–870.
2. Bötel, U., Gläser, E., Niedeggen, A., and Meindl, R. (1997). The cost of ventilator-dependent spinal cord injuries-patients in the hospital and at home. Spinal Cord 35, 40–42.
3. French, D.D., Campbell, R.R., Sabharwal, S., Nelson, A.L., Palacios, P.A., and Gavin-Dreschnack, D. (2007). Health care costs for patients with chronic spinal cord injury in the Veterans Health Administration. J. Spinal Cord Med. 30, 477–481.
4. National Spinal Cord Injury Statistical Center. (2017). Spinal Cord Injury Facts and Figures at a Glance. University of Alabama at Birmingham: Birmingham, AL.
5. Lane, M.A., Lee, K.-Z., Salazar, K., O'Steen, B.E., Bloom, D.C., Fuller, D.D., and Reier, P.J. (2012). Respiratory function following bilateral mid-cervical contusion injury in the adult rat. Exp. Neurol. 235, 197–210.
6. Gill, L.C., Gransee, H.M., Sieck, G.C., and Mantilla, C.B. (2016). Functional recovery after cervical spinal cord injury: role of neurotrophin and glutamatergic signaling in phrenic motoneurons. Respir. Physiol. Neurobiol. 226, 128–136.
7. Darlot, F., Cayetanot, F., Gauthier, P., Matarazzo, V., and Kastner, A. (2012). Extensive respiratory plasticity after cervical spinal cord injury in rats: axonal sprouting and rerouting of ventrolateral bulbospinal pathways. Exp. Neurol. 236, 88–102.
8. Bezdudnaya, T., Marchenko, V., Zholudeva, L.V., Spruance, V.M., and Lane, M.A. (2017). Supraspinal respiratory plasticity following acute cervical spinal cord injury. Exp. Neurol. 293, 181–189.
9. Hoh, D.J., Mercier, L.M., Hussey, S.P., and Lane, M.A. (2013). Respiration following spinal cord injury: evidence for human neuroplasticity. Respir. Physiol. Neurobiol. 189, 450–464.
10. Zholudeva, L.V., Karliner, J.S., Dougherty, K.J., and Lane, M.A. (2017). Anatomical recruitment of spinal V2a interneurons into phrenic motor circuitry after high cervical spinal cord injury. J. Neurotrauma 34, 3058–3065.
11. Lane, M.A., White, T.E., Coutts, M.A., Jones, A.L., Sandhu, M.S., Bloom, D.C., Bolser, D.C., Yates, B.J., Fuller, D.D., and Reier, P.J. (2008). Cervical prephrenic interneurons in the normal and lesioned spinal cord of the adult rat. J. Comp. Neurol. 511, 692–709.
12. Gonzalez-Rothi, E.J., Rombola, A.M., Rousseau, C.A., Mercier, L.M., Fitzpatrick, G.M., Reier, P.J., Fuller, D.D., and Lane, M.A. (2015). Spinal interneurons and forelimb plasticity after incomplete cervical spinal cord injury in adult rats. J. Neurotrauma 32, 893–907.
13. Bareyre, F.M., Kerschensteiner, M., Raineteau, O., Mettenleiter, T.C., Weinmann, O., and Schwab, M.E. (2004). The injured spinal cord spontaneously forms a new intraspinal circuit in adult rats. Nat. Neurosci. 7, 269–277.
14. van den Brand, R., Heutschi, J., Barraud, Q., DiGiovanna, J., Bartholdi, K., Huerlimann, M., Friedli, L., Vollenweider, I., Moraud, E.M., Duis, S., Dominici, N., Micera, S., Musienko, P., and Courtine, G. (2012). Restoring voluntary control of locomotion after paralyzing spinal cord injury. Science 336, 1182–1185.
15. White, T.E., Lane, M.A., Sandhu, M.S., O'Steen, B.E., Fuller, D.D., and Reier, P.J. (2010). Neuronal progenitor transplantation and respiratory outcomes following upper cervical spinal cord injury in adult rats. Exp. Neurol. 225, 231–236.

16. Lin, C.-C., Lai, S.-R., Shao, Y.-H., Chen, C.-L., and Lee, K.-Z. (2017). The therapeutic effectiveness of delayed fetal spinal cord tissue transplantation on respiratory function following mid-cervical spinal cord injury. Neurotherapeutics 14, 792–809.
17. Lee, K.-Z., Lane, M.A., Dougherty, B.J., Mercier, L.M., Sandhu, M.S., Sanchez, J.C., Reier, P.J., and Fuller, D.D. (2014). Intraspinal transplantation and modulation of donor neuron electrophysiological activity. Exp. Neurol. 251, 47–57.
18. Rao, M.S., and Mayer-Proschel, M. (1997). Glial-restricted precursors are derived from multipotent neuroepithelial stem cells. Dev. Biol. 188, 48–63.
19. Mayer-Proschel, M., Kalyani, A.J., Mujtaba, T., and Rao, M.S. (1997). Isolation of lineage-restricted neuronal precursors from multipotent neuroepithelial stem cells. Neuron 19, 773–785.
20. Kalyani, A.J., Piper, D., Mujtaba, T., Lucero, M.T., and Rao, M.S. (1998). Spinal cord neuronal precursors generate multiple neuronal phenotypes in culture. J. Neurosci. 18, 7856–7868.
21. Reier, P.J., Houle, J.D., Jakeman, L., Winialski, D., and Tessler, A. (1988). Transplantation of fetal spinal cord tissue into acute and chronic hemisection and contusion lesions of the adult rat spinal cord. Prog. Brain Res. 78, 173–179.
22. Lane, M.A., Lepore, A.C., and Fischer, I. (2016). Improving the therapeutic efficacy of neural progenitor cell transplantation following spinal cord injury. Expert Rev. Neurother. 17, 433–440.
23. Bonner, J.F., and Steward, O. (2015). Repair of spinal cord injury with neuronal relays: from fetal grafts to neural stem cells. Brain Res. 1619, 115–123.
24. Reier, P.J., Bregman, B.S., and Wujek, J.R. (1986). Intraspinal transplantation of embryonic spinal cord tissue in neonatal and adult rats. J. Comp. Neurol. 247, 275–296.
25. Jakeman, L.B., and Reier, P.J. (1991). Axonal projections between fetal spinal cord transplants and the adult rat spinal cord: a neuroanatomical tracing study of local interactions. J. Comp. Neurol. 307, 311–334.
26. Giovanini, M.A., Reier, P.J., Eskin, T.A., Wirth, E., and Anderson, D.K. (1997). Characteristics of human fetal spinal cord grafts in the adult rat spinal cord: influences of lesion and grafting conditions. Exp. Neurol. 148, 523–543.
27. Anderson, D.K., Howland, D.R., and Reier, P.J. (1995). Fetal neural grafts and repair of the injured spinal cord. Brain Pathol. 5, 451–457.
28. Altman, P.L., and Dittmer, D.S. (1962). Growth, including reproduction and morphological development. Compiled and edited by Philip L. Altman and Dorothy D. Katz. Federation of American Societies for Experimental Biology, Washington, DC.
29. Wirth, E.D., Reier, P.J., Fessler, R.G., Thompson, F.J., Uthman, B., Behrman, A., Beard, J., Vierck, C.J., and Anderson, D.K. (2001). Feasibility and safety of neural tissue transplantation in patients with syringomyelia. J. Neurotrauma 18, 911–929.
30. Bonner, J.F., Haas, C.J., and Fischer, I. (2013). Preparation of neural stem cells and progenitors: neuronal production and grafting applications. Preparation of neural stem cells and progenitors: neuronal production and grafting applications. Methods Mol. Biol. 1078, 65–88.
31. Mori, F., Himes, B.T., Kowada, M., and Murray, M. (1997). Fetal spinal cord transplants rescue some axotomized rubrospinal neurons from retrograde cell death in adult rats. Fetal spinal cord transplants rescue some axotomized rubrospinal neurons from retrograde cell death in adult rats. Exp. Neurol. 143, 45–60.
32. Lepore, A.C., and Fischer, I. (2005). Lineage-restricted neural precursors survive, migrate, and differentiate following transplantation into the injured adult spinal cord. Lineage-restricted neural precursors survive, migrate, and differentiate following transplantation into the injured adult spinal cord. Exp. Neurol. 194, 230–242.
33. Stokes, B.T., and Reier, P.J. (1992). Fetal grafts alter chronic behavioral outcome after contusion damage to the adult rat spinal cord. Exp. Neurol. 116, 1–12.
34. Horner, P.J., Reier, P.J., and Stokes, B.T. (1996). Quantitative analysis of vascularization and cytochrome oxidase following fetal transplantation in the contused rat spinal cord. J. Comp. Neurol. 364, 690–703.
35. Lu, P., Wang, Y., Graham, L., McHale, K., Gao, M., Wu, D., Brock, J., Blesch, A., Rosenzweig, E.S., Havton, L.A., Zheng, B., Conner, J.M., Marsala, M., and Tuszynski, M.H. (2012). Long-distance growth and connectivity of neural stem cells after severe spinal cord injury. Cell 150, 1264–1273.
36. Hou, S., Tom, V.J., Graham, L. and Lu, P. (2013). Partial restoration of cardiovascular function by embryonic neural stem cell grafts after complete spinal cord transection. Partial restoration of cardiovascular function by embryonic neural stem cell grafts after complete spinal cord transection. J. Neurosci. 33, 17138–17149.
37. Harris, J., Lee, H., Tu, C., Cribbs, D., Cotman, C., and Jeon, N. (2007). Preparing E18 cortical rat neurons for compartmentalization in a microfluidic device. J. Vis. Exp. (8), 305.
38. Fuller, D.D., Lee, K.-Z., and Tester, N.J. (2013). The impact of spinal cord injury on breathing during sleep. Respir. Physiol. Neurobiol. 188, 344–354.
39. Bascom, A.T., Sankari, A., Goshgarian, H.G., and Badr, M.S. (2015). Sleep onset hypoventilation in chronic spinal cord injury. Physiol. Rep. 3, e12490.
40. Reier, P.J., Stokes, B.T., Thompson, F.J., and Anderson, D.K. (1992). Fetal cell grafts into resection and contusion/compression injuries of the rat and cat spinal cord. Exp. Neurol. 115, 177–188.
41. Horner, P.J., and Stokes, B.T. (1995). Fetal transplantation following spinal contusion injury results in chronic alterations in CNS glucose metabolism. Exp. Neurol. 133, 231–243.
42. Tessler, A., Himes, B.T., Houle, J., and Reier, P.J. (1988). Regeneration of adult dorsal root axons into transplants of embryonic spinal cord. J. Comp. Neurol. 270, 537–548.
43. Jakeman, L.B., Reier, P.J., Bregman, B.S., Wade, E.B., Dailey, M., Kastner, R.J., Himes, B.T., and Tessler, A. (1989). Differentiation of substantia gelatinosa-like regions in intraspinal and intracerebral transplants of embryonic spinal cord tissue in the rat. Exp. Neurol. 103, 17–33.
44. Sharp, K.G., Yee, K.M., and Steward, O. (2014). A re-assessment of long distance growth and connectivity of neural stem cells after severe spinal cord injury. Exp. Neurol. 257, 186–204.
45. Priest, C.A., Manley, N.C., Denham, J., Wirth, E.D., and Lebkowski, J.S. (2015). Preclinical safety of human embryonic stem cell-derived oligodendrocyte progenitors supporting clinical trials in spinal cord injury. Regen. Med. 10, 939–958.
46. Lepore, A.C., Han, S.S., Tyler-Polsz, C.J., Cai, J., Rao, M.S., and Fischer, I. (2004). Differential fate of multipotent and lineage-restricted neural precursors following transplantation into the adult CNS. Neuron Glia Biol. 1, 113–126.
47. Cai, J., Wu, Y., Mirua, T., Pierce, J.L., Lucero, M.T., Albertine, K.H., Spangrude, G.J., and Rao, M.S. (2002). Properties of a fetal multipotent neural stem cell (NEP cell). Dev. Biol. 251, 221–240.
48. Golding, J.P., and Cohen, J. (1997). Border controls at the mammalian spinal cord: late-surviving neural crest boundary cap cells at dorsal root entry sites may regulate sensory afferent ingrowth and entry zone morphogenesis. Mol. Cell. Neurosci. 9, 381–396.
49. Bregman, B.S., and Reier, P.J. (1986). Neural tissue transplants rescue axotomized rubrospinal cells from retrograde death. J. Comp. Neurol. 244, 86–95.
50. Houlé, J.D., and Reier, P.J. (1988). Transplantation of fetal spinal cord tissue into the chronically injured adult rat spinal cord. J. Comp. Neurol. 269, 535–547.
51. Vescovi, A.L., Galli, R., and Reynolds, B.A. (2006). Brain tumour stem cells. Nat. Rev. Cancer 6, 425–436.
52. Reynolds, B.A., and Weiss, S. (1992). Generation of neurons and astrocytes from isolated cells of the adult mammalian central nervous system. Science 255, 1707–1710.
53. Nottebohm, F. (2004). The road we travelled: discovery, choreography, and significance of brain replaceable neurons. Ann. N. Y. Acad. Sci. 1016, 628–658.
54. Altman, J., and Das, G.D. (1965). Autoradiographic and histological evidence of postnatal hippocampal neurogenesis in rats. J. Comp. Neurol. 124, 319–335.
55. Dhillon, A.S., Hagan, S., Rath, O., and Kolch, W. (2007). MAP kinase signalling pathways in cancer. Oncogene 26, 3279–3290.
56. Riess, P., Molcanyi, M., Bentz, K., Maegele, M., Simanski, C., Carlitscheck, C., Schneider, A., Hescheler, J., Bouillon, B., Schäfer, U., and Neugebauer, E. (2007). Embryonic stem cell transplantation after experimental traumatic brain injury dramatically improves neurological outcome, but may cause tumors. J. Neurotrauma 24, 216–225.
57. Amariglio, N., Hirshberg, A., Scheithauer, B.W., Cohen, Y., Loewenthal, R., Trakhtenbrot, L., Paz, N., Koren-Michowitz, M., Waldman, D., Leider-Trejo, L., Toren, A., Constantini, S., and Rechavi, G. (2009). Donor-derived brain tumor following neural stem cell transplantation in an ataxia telangiectasia patient. PLoS Med. 6, e1000029.

58. Tuszynski, M.H., Wang, Y., Graham, L., McHale, K., Gao, M., Wu, D., Brock, J., Blesch, A., Rosenzweig, E.S., Havton, L.A., Zheng, B., Conner, J.M., Marsala, M., and Lu, P. (2014). Neural stem cells in models of spinal cord injury. Exp. Neurol.. 261, 494–500.
59. Reier, P.J., Perlow, M.J., and Guth, L. (1983). Development of embryonic spinal cord transplants in the rat. Brain Res. 312, 201–219.
60. Nógrádi, A., and Nógrádi, A. (2006). *Transplantation of Neural Tissue into the Spinal Cord*. Springer Science+Business Media: New York, NY.
61. Houle, J. (1992). The structural integrity of glial scar tissue associated with a chronic spinal cord lesion can be altered by transplanted fetal spinal cord tissue. J. Neurosci. Res. 31, 120–130.
62. Sternfeld, M.J., Hinckley, C.A., Moore, N.J., Pankratz, M.T., Hilde, K.L., Driscoll, S.P., Hayashi, M., Amin, N.D., Bonanomi, D., Gifford, W.D., Sharma, K., Goulding, M., and Pfaff, S.L. (2017). Speed and segmentation control mechanisms characterized in rhythmically-active circuits created from spinal neurons produced from genetically-tagged embryonic stem cells. eLife 6, e21540.
63. Alaynick, W.A., Jessell, T.M., and Pfaff, S.L. (2011). SnapShot: spinal cord development. Cell 146, 178–1780.
64. Phelps, P.E., Barber, R.P., Houser, C.R., Crawford, G.D., Salvaterra, P.M., and Vaughn, J.E. (1984). Postnatal development of neurons containing choline acetyltransferase in rat spinal cord: an immunocytochemical study. J. Comp. Neurol. 229, 347–361.
65. Barber, R.P., Phelps, P.E., Houser, C.R., Crawford, G.D., Salvaterra, P.M., and Vaughn, J.E. (1984). The morphology and distribution of neurons containing choline acetyltransferase in the adult rat spinal cord: an immunocytochemical study. J. Comp. Neurol. 229, 329–346.
66. Francius, C., Harris, A., Rucchin, V., Hendricks, T.J., Stam, F.J., Barber, M., Kurek, D., Grosveld, F.G., Pierani, A., Goulding, M., and Clotman, F. (2013). Identification of multiple subsets of ventral interneurons and differential distribution along the rostrocaudal axis of the developing spinal cord. PLoS One 8, e70325.
67. Lu, D.C., Niu, T., and Alaynick, W.A. (2015). Molecular and cellular development of spinal cord locomotor circuitry. Front. Mol. Neurosci. 8, 25.
68. Miles, G.B., Hartley, R., Todd, A.J., and Brownstone, R.M. (2007). Spinal cholinergic interneurons regulate the excitability of motoneurons during locomotion. Proc. Natl. Acad. Sci. U. S. A. 104, 2448–2453.
69. Adler, A.F., Lee-Kubli, C., Kumamaru, H., Kadoya, K., and Tuszynski, M.H. (2017). Comprehensive monosynaptic rabies virus mapping of host connectivity with neural progenitor grafts after spinal cord injury. Stem Cell Rep. 8, 1525–1533.
70. Gonzalez-Rothi, E.J., Lee, K.-Z.Z., Dale, E.A., Reier, P.J., Mitchell, G.S., and Fuller, D.D. (2015). Intermittent hypoxia and neurorehabilitation. J. Appl. Physiol. 119, 1455–1465.
71. Alilain, W.J., Horn, K.P., Hu, H., Dick, T.E., and Silver, J. (2011). Functional regeneration of respiratory pathways after spinal cord injury. Nature 475, 196–200.
72. Hoffman, M.S., and Mitchell, G.S. (2011). Spinal 5-HT7 receptor activation induces long-lasting phrenic motor facilitation. J. Physiol. 589, 1397–1407.
73. Lee, K.-Z., and Gonzalez-Rothi, E.J. (2017). Contribution of 5-HT2A receptors on diaphragmatic recovery after chronic cervical spinal cord injury. Respir. Physiol. Neurobiol. 244, 51–55.
74. Choi, H., Liao, W.-L., Newton, K.M., Onario, R.C., King, A.M., Desilets, F.C., Woodard, E.J., Eichler, M.E., Frontera, W.R., Sabharwal, S., and Teng, Y.D. (2005). Respiratory abnormalities resulting from midcervical spinal cord injury and their reversal by serotonin 1A agonists in conscious rats. J. Neurosci. 25, 4550–4559.
75. Hormigo, K.M., Zholudeva, L.V., Spruance, V.M., Marchenko, V., Cote, M.-P., Vinit, S., Giszter, S., Bezdudnaya, T., and Lane, M.A. (2017). Enhancing neural activity to drive respiratory plasticity following cervical spinal cord injury. Exp. Neurol. 287, 276–287.
76. Golder, F.J., and Mitchell, G.S. (2005). Spinal synaptic enhancement with acute intermittent hypoxia improves respiratory function after chronic cervical spinal cord injury. J. Neurosci. 25, 2925–2932.
77. Hayes, H.B., Jayaraman, A., Herrmann, M., Mitchell, G.S., Rymer, W.Z., and Trumbower, R.D. (2014). Daily intermittent hypoxia enhances walking after chronic spinal cord injury: a randomized trial. Neurology 82, 104–113.
78. Trumbower, R.D., Jayaraman, A., Mitchell, G.S., and Rymer, W.Z. (2012). Exposure to acute intermittent hypoxia augments somatic motor function in humans with incomplete spinal cord injury. Neurorehabil. Neural Repair 26, 163–172.
79. Kinkead, R., Bach, K.B., Johnson, S.M., Hodgeman, B.A., and Mitchell, G.S. (2001). Plasticity in respiratory motor control: intermittent hypoxia and hypercapnia activate opposing serotonergic and noradrenergic modulatory systems. Comp. Biochem. Physiol. A Mol. Integr. Physiol. 130, 207–218.
80. Iyer, N.R., Wilems, T.S., and Sakiyama-Elbert, S.E. (2017). Stem cells for spinal cord injury: Strategies to inform differentiation and transplantation. Biotechnol. Bioeng. 114, 245–259.
81. Butts, J.C., McCreedy, D.A., Martinez-Vargas, J.A., Mendoza-Camacho, F.N., Hookway, T.A., Gifford, C.A., Taneja, P., Noble-Haeusslein, L., and McDevitt, T.C. (2017). Differentiation of V2a interneurons from human pluripotent stem cells. Proc. Natl. Acad. Sci. U. S. A. 114, 4969–4974.
82. Xu, H., and Sakiyama-Elbert, S.E. (2015). Directed differentiation of V3 interneurons from mouse embryonic stem cells. Stem Cells Dev. 24, 2723–2732.
83. Cregg, J.M., Chu, K.A., Dick, T.E., Landmesser, L.T., and Silver, J. (2017). Phasic inhibition as a mechanism for generation of rapid respiratory rhythms. Proc. Natl. Acad. Sci. U. S. A. 114, 12815–12820.
84. Cregg, J.M., Chu, K.A., Hager, L.E., Maggard, R.S., Stoltz, D.R., Edmond, M., Alilain, W.J., Philippidou, P., Landmesser, L.T., and Silver, J. (2017). A latent propriospinal network can restore diaphragm function after high cervical spinal cord injury. Cell Rep. 21, 654–665.
85. Wu, J., Capelli, P., Bouvier, J., Goulding, M., Arber, S., and Fortin, G. (2017). A V0 core neuronal circuit for inspiration. Nat. Commun. 8, 544.

Address correspondence to:
Michael A. Lane, PhD
Department of Neurobiology and Anatomy
Spinal Cord Research Center
Drexel University College of Medicine
2900 West Queen Lane
Philadelphia, PA 19129

E-mail: mlane.neuro@gmail.com